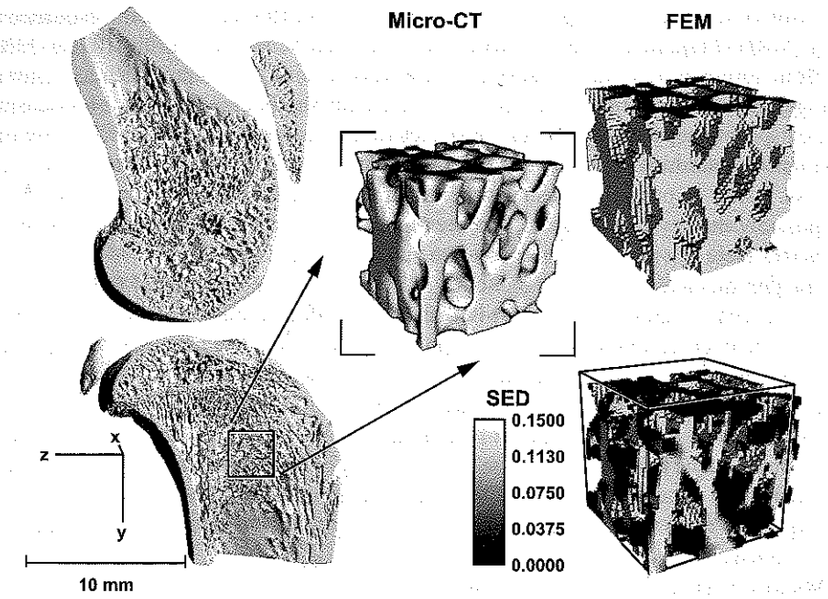

Figure 2.3.9 **High resolution computed tomography (micro-CT) of a cat femur (left; adapted from Boyd et al., 2005) with a small region of interest extracted (middle). After conversion to a finite element model (top right), the deformation and the strain energy density can be determined for a given load (bottom right).**

chitecture is that the measurements are restricted to peripheral limbs, i.e., distal radius or distal tibia, where signal-to-noise ratios can be maximized. Nevertheless, these tools offer exciting new potential for learning about bone quality in patients, and they are poised to become important options for improving bone-related health care.

2.4 ARTICULAR CARTILAGE

HERZOG, W.
FEDERICO, S.

2.4.1 INTRODUCTION

Articular cartilage is a thin (about 1 to 6 mm in human joints) layer of fibrous connective tissue covering the articular surfaces of bones in synovial joints (Figure 2.4.1). It consists of cells (2 to 15% in terms of volumetric fraction) and an intercellular matrix (85 to 98%) with 65 to 80% water content. Articular cartilage is a viscoelastic material that, in conjunction with synovial (joint) fluid, allows for virtually frictionless movement (coefficients of friction range from 0.002 to 0.05) of the joint surfaces. The primary functions of articular cartilage include:

- Transmitting force across joints,
- Distributing articular forces to minimize stress concentrations, and
- Providing a smooth surface for relative gliding of joint surfaces.

Osteoarthritis is a joint disease that is associated with a degradation and loss of articular cartilage from the joint surfaces and an associated increase in joint friction causing pain and disability, particularly in the elderly population. In most people, articular cartilage fulfills its functional role for decades, although the incidence of osteoarthritis in North America is about 50% among people of age 60 and greater.

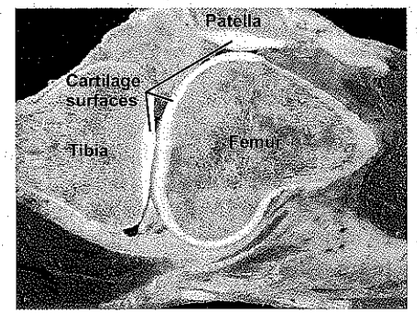

Figure 2.4.1 **Sagittal plane section through a human knee showing the femur, tibia, and patella, and associated articular cartilage.**

2.4.2 STRUCTURE

Articular cartilage is structurally heterogeneous, and material properties change as a function of depth. Although these changes are continuous, articular cartilage is typically di-

vided into four structural zones.

The four structural zones of articular cartilage (Figure 2.4.2) are:

- Superficial zone,
- Middle (or transitional) zone,
- Deep (or radial) zone, and
- Calcified zone.

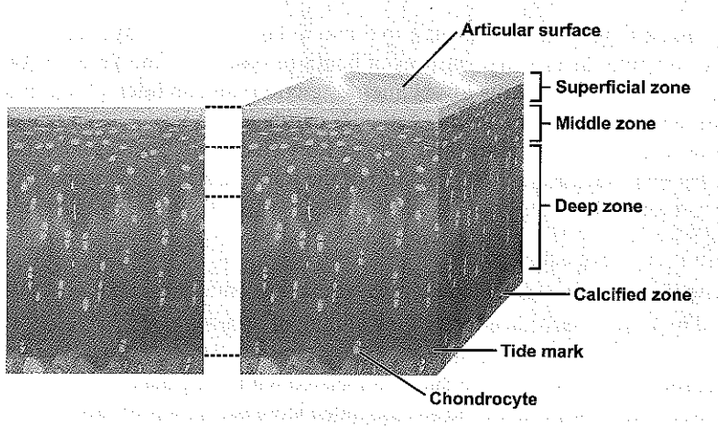

Figure 2.4.2 **The four zones of articular cartilage. The superficial zone provides the sliding surface of joints with collagen fibrils aligned parallel to the surface, and flat, relatively metabolically inactive cells. The middle (or transitional) zone contains collagen fibrils that are oriented randomly, and cells are nearly spherical. The deep (or radial) zone contains collagen fibrils that are oriented perpendicular to the subchondral bone (and articular surface), and the cells are typically aligned in radial columns. The calcified zone provides a mechanical transition that separates the relatively soft cartilage tissue from the stiff subchondral bone.**

The *superficial zone* is the thinnest, most superficial region that forms the gliding surface of joints. It contains a surface layer (lamina splendens) of about 2μm thickness, which is made up of randomly aligned collagen fibrils, and a deep layer consisting of collagen fibrils aligned parallel to the cartilage surface following the so-called "split line pattern" (Hultkrantz, 1898), which follows the direction of normal joint movement.

The collagen fibrils in the superficial zone show a wave-like pattern referred to as crimp. This waving or crimping shows dips and ridges in the μm range (Dowson, 1990). The surface, although apparently smooth to touch and with a low friction coefficient, is not quite smooth at a microscopic level.

The deep layer of the superficial zone contains articular cartilage cells (chondrocytes) that are flat (Hunziker, 1992) and metabolically relatively inactive (Wong et al., 1996), as evidenced by a low content of mitochondria, Golgi organs, and endoplasmic reticula. The deep layer of the superficial zone also contains little proteoglycan, but has the highest water concentration (about 80%) of all zones, as water content decreases with depth to a value of about 65% in the deep zone (Maroudas, 1975; Torzilli, 1985).

The *middle (or transitional) zone* is typically thicker than the superficial zone. Collagen fibrils have a greater diameter in this zone than the superficial zone and are oriented in a nearly random fashion. Proteoglycan content is greater and aggregate complexes are larger than in the superficial zone. Chondrocytes are nearly spherical in this zone and contain great numbers of mitochondria, Golgi bodies, and a vast endoplasmic reticulum network, suggesting that cells in this zone are metabolically more active than those of the superficial zone.

The *deep (or radial) zone* contains the largest diameter collagen fibrils, which are oriented perpendicular to the subchondral bone and the cartilage surface. Water content is lowest and proteoglycan content is typically highest in this zone. The chondrocytes tend to be aligned in radial columns and contain intracytoplasmic filaments, glycogen granules, endoplasmic reticula, and Golgi bodies, suggesting great protein synthesis activity. Benninghof (1925) proposed that collagen fibres form arcades that extend from the deep to the superficial zone, and recent studies confirmed that collagen fibres, indeed, might be continuous through the various cartilage zones (Notzli & Clark, 1997).

The *calcified zone* provides a mechanical transition that separates the relatively soft cartilage tissue and the stiff subchondral bone. It is characterized by hydroxyapatite, an inorganic constituent of bone matrix. The calcified zone is separated from the deep (radial) zone by the *tidemark*, an undulating line that is a few μm thick. Collagen fibres from the deep zone cross the tidemark and anchor into the calcified zone, thereby strongly adhering cartilage to bone. The calcified zone contains metabolically active chondrocytes, serves for structural integration, and has been considered important for nutrition and cartilage repair arising from the underlying bone (Hunziker, 1992).

The structural differences across the various zones of articular cartilage have been thought to be the primary cause for the anisotropy of articular cartilage (e.g., Schinagl et al., 1997) and have motivated structural models of transverse isotropic cartilage models (Federico et al., 2005).

2.4.3 COMPOSITION

Articular cartilage consists mostly (85 to 98%) of matrix and a sparse population of cells (about 2 to 15% in terms of volumetric fraction). It is avascular, aneural, and alymphatic.

CELLS

Chondrocytes are metabolically active cells that are responsible for the synthesis and degradation of the matrix. They are isolated, lie in lacunae, and receive nourishment through diffusion of substrates that is thought to be facilitated by cycling loading and unloading, which is common for many articular joint surfaces. As described above, the volumetric fraction, shape, and metabolic activity of cells varies as a function of location, varies across cartilages in different joints, and even varies within the same joint at different locations, e.g., Stockwell (1979); Muir (1983); Clark et al. (2005). It is accepted that normal loading of articular cartilage produces deformations in chondrocytes and the corresponding cell nuclei (Guilak, 1995; Guilak et al., 1995). These deformations have been thought responsible for the biosynthetic activity of cells. In general, static, long-lasting loads have

been associated with a tissue degrading response, while dynamic loading of physiological magnitudes has been related to positive adaptive responses.

Chondrocytes are softer than the surrounding extracellular matrix by a factor of about 1000x. Therefore, chondrocytes can be expected to be deformed much more during loading than the matrix, and might even be expected to collapse. However, chondrocytes are surrounded by a protective cover that consists of a pericellular matrix and a pericellular capsule (Poole et al., 1997). The chondrocyte and its pericellular matrix and capsule constitute the chondron, which is the primary functional and metabolic unit of cartilage. It has been suggested that the chondron acts hydrodynamically to protect the chondrocytes from excessive stresses and strains during cartilage compression. Chondrocytes in different types of cartilages have different functional and metabolic roles. In articular cartilage, chondrocytes specialize in producing type II collagen and proteoglycan.

MATRIX

The intercellular *matrix* of articular cartilage is largely responsible for the functional and mechanical properties associated with this tissue. It consists of structural macromolecules and tissue fluid. Fluid comprises between 65 to 80% of the wet weight of articular cartilage, and its volumetric fraction decreases from the superficial to the deep zone. Macromolecules, which are produced by the chondrocytes, comprise 20 to 40%. Of the macromolecules, collagens contribute about 50% of the tissue dry weight. Proteoglycans contribute approximately 30 to 35% and non-collagenous proteins/glycoproteins contribute 15 to 20% of the tissue dry weight (Buckwalter et al., 1991). The interactions of tissue fluid with the structural macromolecules give articular cartilage its specific mechanical and electro-static properties. As the distribution, orientation and density of these macromolecules changes with cartilage depth, so do the functional and material properties of the tissue.

Collagen

There are at least 18 different types of *collagen*. However, in articular cartilage, type II collagen is by far the most abundant (about 80 to 85% of all collagens). Other types of collagen (V, VI, IX, X and XI) are also found in articular cartilage and have been associated with specific functional roles (Thomas et al., 1994; Hasler et al., 1999). Collagen molecules are comprised of three α-chains that are interwoven in a helical configuration. Each chain has a high hydroxylysine content and covalently bound carbohydrates that make it adhere readily with proteoglycans.

Collagens have a high tensile stiffness (about 2 to 46 MPa for uncross-linked type I collagen from rat tail tendon and 380 to 770 MPa when cross-linked (Pins et al., 1997)). Because of their fibrillar structure, collagens are typically thought to have negligible compressive strength, as they are assumed to buckle when subjected to compressive loading (Li et al., 2000a; Soulhat et al., 1999). However, some scientists think of collagen fibrils as reinforced inclusions (similar to steel rods embedded in concrete) with appreciable compressive capabilities, and thereby contributing substantially to withstand compressive forces (Wu & Herzog, 2002). Collagens form a structural network that gives cartilage its tensile strength. Because of the characteristic orientation of the fibrillar network, collagens are associated with providing resistance to compressive loading, as fluid pressurization tends to load the collagen network in tension. Collagen fibrils are cross-linked for further strength (Pins et al., 1997), and are connected to proteoglycans via molecular chains arising from glycosaminoglycans and polysaccharides. Thus, collagens are intimately associated with other macromolecules and so make up a tough tissue that, despite its thinness, can withstand high repetitive loading for a lifetime.

Proteoglycans

Proteoglycans are large molecules composed of a central core protein with glycosaminoglycan side chains covalently attached. The protein core makes up about 10% of the molecular weight of proteoglycan, with the side chains making up about the remaining 90%. The glycosaminoglycan side chains contain sugars, which have a negative electrostatic charge, on a protein core. These negatively charged molecules repel each other and attempt to occupy as much volume as possible. Proteoglycans are kept from dissolving into the fluid and being swept away by their attachment to the stretched collagen network. The negative charges are thus forced to stay in close proximity When subjected to external compressive loads, proteoglycans are further compressed and the repulsive forces increase from their natural pre-tensed state.

Articular cartilage contains large aggregating proteoglycans (aggrecan and versican) and small interstitial proteoglycans (biglycan, decorin, fibromodulin, and lumican). The large proteoglycans contribute 50 to 85% of the total proteoglycan content. Aggrecan is the major proteoglycan. Aggrecan consists of a core protein and up to 150 chondroitin and keratin sulphate chains (Figure 2.4.3). The core protein's N-terminal G1 domain interacts with

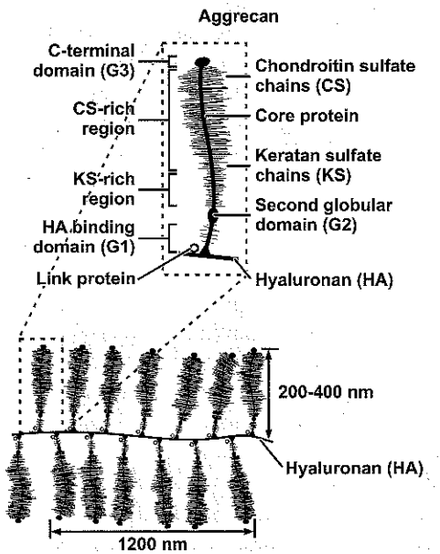

Figure 2.4.3 **Macromolecular aggregate formed by aggrecan molecules (inset-blown up) binding to a chain of hyaluronan through a link protein. The aggrecan molecule consists of a core protein with several domains: hyaluronan binding G1 domain, G2 domain, keratin sulphate rich region, chondroitin sulphate rich region, and C-terminal domain, G3.**

link proteins and hyaluronan, and these three components form stable macromolecular complexes (Figure 2.4.3).

Changes in proteoglycan structure and decreased density often accompany articular cartilage degeneration and aging (Lark et al., 1997; Buckwalter et al., 1985). These changes are typically accompanied by a corresponding increase in water content, decreased stiffness, and reduced resistance to withstand mechanical loading.

Non-collagenous proteins

Non-collagenous proteins play a role in the assembly and integrity of the extracellular matrix, and form links between the chondrocytes and the matrix. Non-collagenous proteins include adhesive glycoproteins such as fibronectin, thrombospondin, chondroadherin, and other matrix proteins such as the link protein, cartilage matrix oligomeric protein, cartilage matrix protein, and proline arginine-rich and leucine-rich repeat proteins. The detailed function of many of these non-collagenous proteins is, currently, not well understood.

Fluid

Articular cartilage tissue *fluid* consists of water and dissolved gas, small proteins and metabolites. Water is the most abundant component of cartilage and accounts for 65 to 80% of its wet weight. Fluid is moved around in articular cartilage, and is closely associated with the synovial fluid of the joint.

Fluid in articular cartilage is intimately associated with the proteoglycan network, which hinders its movement to a certain degree. This arrangement makes cartilage sponge-like in that water is restrained, but, with pressure caused by cartilage loading, will flow with the pressure gradient. When modelling articular cartilage, fluid flow is described by permeability, which is a measure of how easily a fluid flows through a porous material. Permeability is inversely proportional to the force required for a fluid to flow at a given speed through the tissue. Permeability in cartilage is low. Therefore, fluid flow in cartilage is typically small, and any substantial exchange of tissue fluid and synovial fluid, or any significant loss of fluid caused by cartilage compression takes a long time (in the order of minutes). Compared to the typical loading cycle of cartilage in a joint, e.g., about 0.5 seconds of loading during a step cycle, fluid flow is minimal. Therefore, cartilage maintains its stiffness well when loaded, and fluid takes up a big part of the forces in the tissue during physiological (quick) loading cycles, thereby presumably protecting the matrix (and, in turn, the cells) from stresses and strains during normal everyday loading cycles.

Synovial fluid provides lubrication to joints. It is transparent, alkaline and viscous, and is secreted by the synovial membranes, which are contained in joints. Synovial fluid is a dialysate of blood containing hyaluronic acid. Synovial fluid is viscous and contains a glycoprotein called lubricin that is found on the articular surfaces of joints, but not within the cartilage tissue. Cartilage surfaces are physically separated by a 0.5 to 1.0μm film of synovial fluid. Synovial fluid is essential for the mechanical sliding characteristics of joints, and permits the diffusion of gases, nutrients and waste products, thereby making it essential for tissue health.

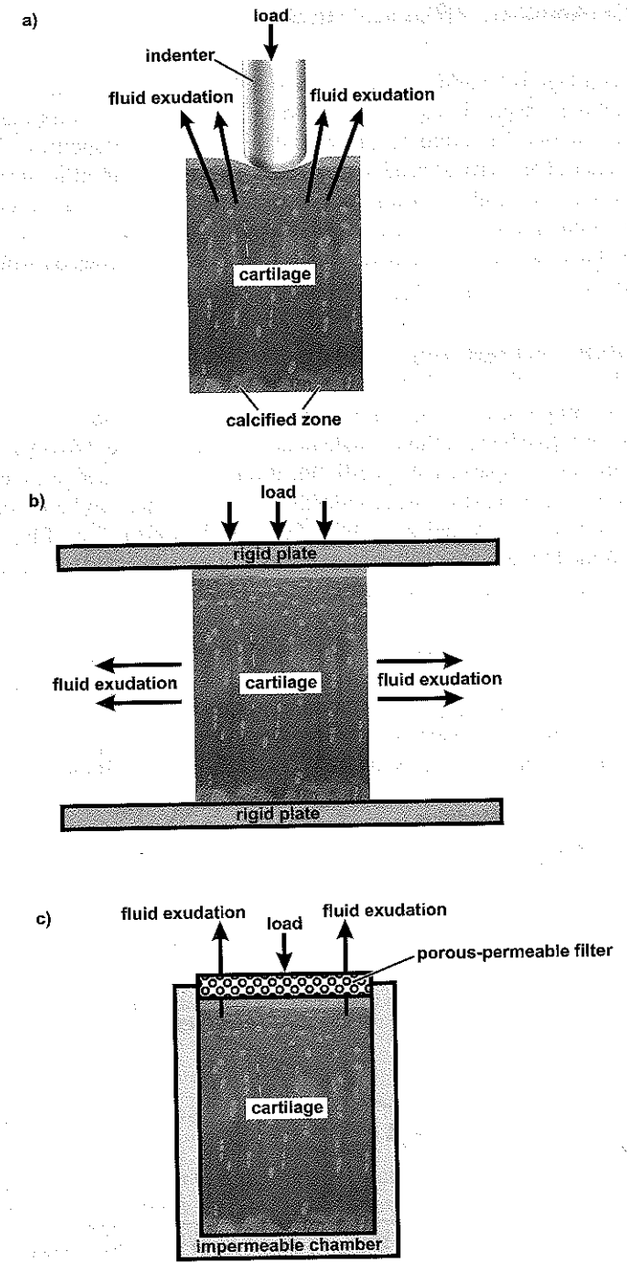

Figure 2.4.4 **Schematic illustration of the three most commonly used techniques for determining articular cartilage mechanical properties: (a) indentation testing, (b) unconfined compression, and (c) confined compression.**

2.4.4 MECHANICAL PROPERTIES

Articular cartilage is a passive structural tissue whose primary functions are mechanical. These functions are providing a smooth sliding surface, and transmitting and distributing forces across joints. Therefore, to understand the functional properties of this tissue, its mechanical (material properties) need to be known. This is insofar difficult as articular cartilage structure and composition varies from one joint to the next, its properties also change with location within a joint, and even across its depth. Nevertheless, many attempts have been made to elucidate the compressive, tensile and shear properties of articular cartilage using a variety of engineering testing approaches.

COMPRESSIVE PROPERTIES

Compressive properties of articular cartilage have not been obtained for the whole tissue attached to its native bone, although indentation testing (Figure 2.4.4a) has been used to evaluate compressive properties at specific locations using exposed joint surfaces, (e.g., Clark et al., 2003), or in patients using indentation devices that can be introduced arthroscopically into joints, e.g., Dashefsky (1987); Lyyra et al. (1995). Typically, material properties are determined for articular cartilage explants that are subjected to unconfined or confined compression testing (Figure 2.4.4b,c)

Compressive properties, elastic modulus and stiffness of a given sample of articular cartilage vary with depth in the tissue. For example, Schinagl et al. (1997) report a more than 20-fold increase in the compressive modulus across the full thickness of bovine articular cartilage tested in unconfined compression. Compressive strength is directly related to proteoglycan concentration, and so is the tissue's compressive stiffness (Figure 2.4.5).

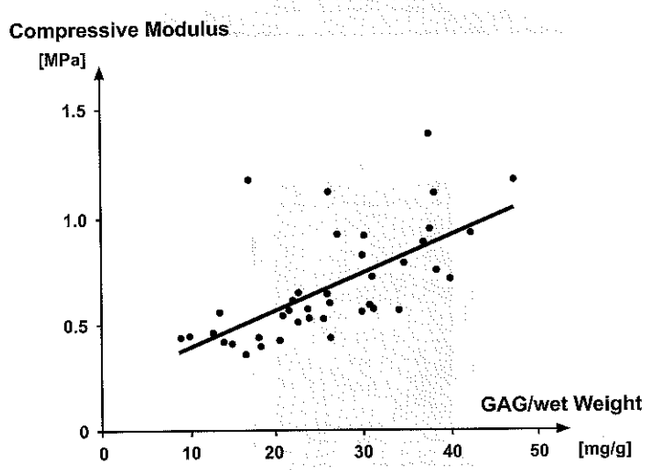

Figure 2.4.5 **Compressive modulus of elasticity as a function glycosaminoglycan (GAG) concentration. Since GAG concentration increases with cartilage depth, so does the tissue's compressive stiffness. Adapted from Sah et al. (1997), with permission.**

Since proteoglycan concentration is known to increase with depth, this result can be expected. However, even a five-fold increase in proteoglycan concentration is only associated with a doubling or tripling of the compressive modulus (Figure 2.4.5). Therefore, it appears that the great changes in stiffness observed experimentally in different cartilage layers must have an additional explanation. One such explanation might be the orientation of the collagen fibrillar network, assuming that the collagen network helps resist compressive loading.

TENSILE PROPERTIES

Articular cartilage functions as a compressive load absorber. However, when loaded, tensile forces are thought to act on the collagen network. Therefore, an understanding of the tensile properties might be important in understanding the functioning of cartilage in vivo. Tensile strength in articular cartilage is highest in the superficial zone and decreases continuously with increasing depth in the tissue (Figure 2.4.6), likely because of variations in the orientation of collagen fibrils, the cross-linking of collagen fibrils, and the ratio of collagen to proteoglycan. Tensile properties are also direction-dependent. When testing occurs along the split line, i.e., along the predominant orientation of the long axis of collagen fibrils, tensile strength and the tensile modulus are greater than when testing is performed perpendicular to the split line (Figure 2.4.6).

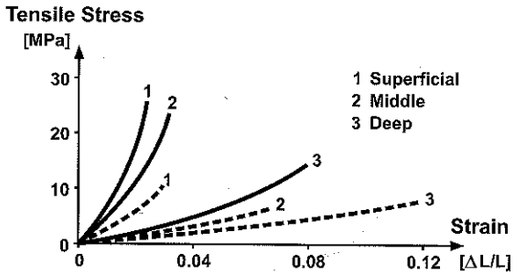

Figure 2.4.6 **Stress-strain curves for tensile testing of articular cartilage specimens from the superficial (1), middle (2), and deep zone (3), and along the long axis of the collagen fibrils (solid lines) and perpendicular to the long axis of the collage fibrils (dashed lines). Tensile strength decreases continuously from the surface to the deep zone and is greater along the collagen fibril direction than perpendicular to it. Adapted from Kempson (1972), with permission.**

SHEAR PROPERTIES

Shear properties in articular cartilage are not well understood, and shear testing is associated with numerous problems. For example, the smoothness of the surface layer makes it difficult to apply shear loads without slippage. Shear testing has become important for identifying flow-independent viscoelasticity of the tissue, as ideally, small deformation shear testing is accomplished with a constant volume and no fluid flow. Shear resistance is thought to come primarily from the collagen network. Consistent with that idea, shear modulus is decreased with decreasing collagen content, as may occur in cartilage diseases such

as osteoarthritis. In addition, because the proteoglycan network is thought to pre-stress the collagen network, loss of pre-stress caused by loss of proteoglycans has also been found to decrease the dynamic and equilibrium shear properties (Zhu et al., 1993).

VISCOELASTICITY

If a material's response to a constant force or deformation varies in time, its mechanical behaviour is said to be viscoelastic, in contrast to an elastic material's response that does not vary in time. Articular cartilage is known to be viscoelastic (Figure 2.4.7), however, the origin for this property remains controversial. Most people agree that one aspect of the viscoelastic behaviour is associated with fluid flow, and some believe that there is also a flow-independent viscoelasticity that resides in the matrix proper. Since fluid flow is proportional to the pore pressure gradient in water, fluid flow can be described by the coefficient of hydraulic permeability. The inverse of this coefficient gives a measure of the material's resistance to fluid flow. Since proteoglycans attempt to restrain fluid flow, permeability is smallest in areas with high proteoglycan concentration, e.g., deep layers, and cartilage is most permeable in zones of low proteoglycan concentration, e.g., the surface layer.

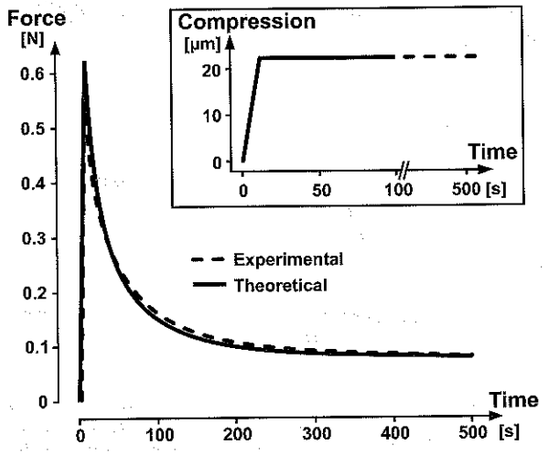

Figure 2.4.7 **Experimental and theoretical force-relaxation curve for articular cartilage exposed to unconfined ramp loading (as shown in the inset). Articular cartilage exhibits a typical viscoelastic response that is associated with fluid flow, and possibly also with an inherent viscoelasticity of the matrix component.**

2.4.5 BIOMECHANICS

The material properties of articular cartilage are of great importance because of articular cartilage's roles in transmitting and distributing force across joints, and providing a smooth surface for virtually frictionless gliding. However, articular cartilage is only one component of a joint, and to understand articular cartilage biomechanics, the functional requirements of articular cartilage within the "organ" joint need to be known. Malfunctioning

of one component of a joint (for example, a breakdown of the articular cartilage, loss of a guiding ligament, or rupture of a meniscal inclusion) will affect all structures of a joint. Therefore, focusing on a single component might not do justice to the intricate functionality of that component in its native environment.

When a joint moves, the articular surfaces slide relative to one another, the size and location of the contact area changes, and the contact pressure distribution is affected by the changing surface geometry and the variable forces applied to the joint. In addition, for a given joint configuration, that is a given orientation of the articular surfaces, the contact area increases with increasing force transmission across the joint. For example, the cat patellofemoral joint contact area increases with increasing force potential of the quadriceps muscles, thereby providing a natural way for keeping average pressure between the contacting surfaces low when forces become big. Similarly, when forces transmitted across the patellofemoral joint are increased by a factor of five (from 100 to 500N), the contact area increases by a factor of about four (from about 7 to about 30 mm^2), while the mean contact pressure only increases by a factor of about 0.6 [from 7.7 to 12.9MPa (Figure 2.4.8)].

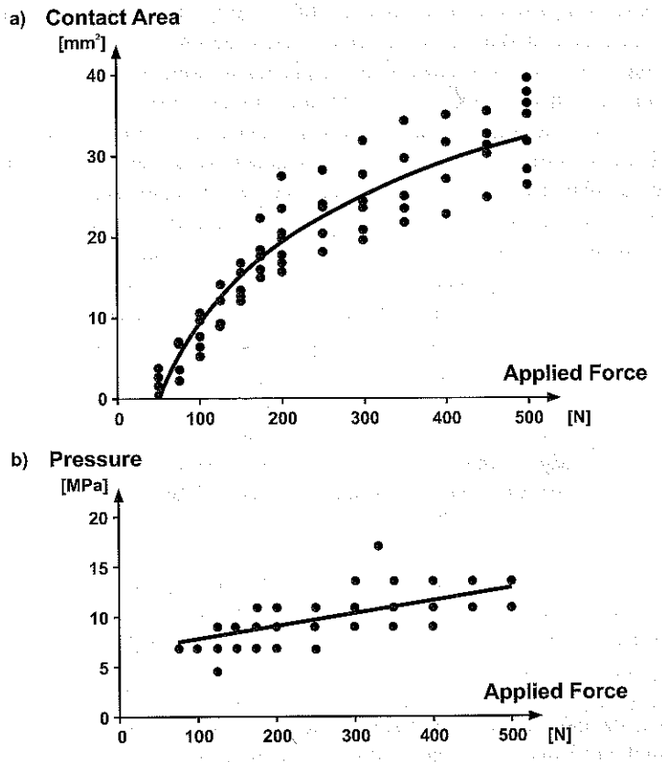

Figure 2.4.8 **Feline patellofemoral contact area (a) and peak pressure (b) transmitted across the joint. Contact area increases quickly with increasing force, especially in the range of physiological loading (0 to 200 N), while peak pressures are less sensitive to changes in joint loading.**

Therefore, contact pressures on the articular surfaces of joints are kept small with increasing forces by increasing:

- Contact areas for joint angles where large muscular forces are possible, and
- Contact area as a function of the applied forces through the viscoelastic properties of articular cartilage.

The loads transmitted across joint surfaces are not well known, because most of the loading in joints is caused by muscles. Muscle forces are hard to measure in vivo and cannot be estimated accurately and reliably. However, Rushfeldt et al. (1981a; 1981b) developed techniques to measure local hip joint contact pressures by mounting pressure transducers on an endoprosthesis that replaced the natural femoral head. They measured average articular surface pressures in the joint of about 2 to 3 MPa, with peak pressures reaching 7 MPa, for loads equivalent to the single stance phase of walking (2.6 times body weight). Peak hip joint pressures reached were in the range of 18 MPa and were obtained for walking downstairs and rising from a chair (Mann, 2005). Using telemetry-based force measurements from patients with total hip joint replacements, Bergmann et al. (1993) measured resultant hip forces of 2.8 to 4.8 times body weight for walking at speeds ranging from 1 to 5 km per hour. Very fast walking or slow running increased these forces to about 5.5 times body weight, while stumbling (unintentionally) gave temporary peak resultant hip joint forces of 7.2 and 8.7 times body weight in two patients. No corresponding joint pressure or force data are available for intact human joints during normal everyday movements.

Similarly, direct pressure measurements in an intact diarthrodial joint during unrestrained movements are not available from animal experimentation. However, quadriceps forces and the corresponding knee kinematics have been measured in freely walking cats. Joint pressure distributions could then be obtained using Fuji pressure-sensitive film in the anaesthetized animals while reproducing the joint angles and muscle forces observed during locomotion. Average peak pressures obtained by using this approach were 5.7 MPa in the patellofemoral joint. When the quadriceps muscles were fully activated (through electrical stimulation), median pressure in the cat patellofemoral joint reached 11 MPa, and peak pressure reached 47 MPa, indicating that joint pressures in normal everyday movements are much smaller than can be produced by maximal muscle contraction (Hasler and Herzog, 1998).

The forces transmitted by articular cartilage across leg joints are in the order of several times body weight for normal everyday tasks such as walking, getting up from a chair, and walking up or down stairs. The corresponding articular surface pressures range from about 2 to 10 MPa, but maximal muscle contraction can produce peak pressures in knee articular cartilage of almost 50 MPa. Such high pressures, when applied to articular cartilage explants through confined or unconfined compression, cause cell death and matrix damage, and also cause damage when applied to the whole joint through impact (peak pressures attained within 0.5 to 3 ms). Muscular loading of the intact joint does not cause articular cartilage damage, indicating that the time of load application (typically more than 100 ms for human muscles), joint integrity and articular surface movements during force production provide a safe environment for high cartilage loading that is lost when testing articular cartilage explants in vitro.

2.4.6 OSTEOARTHRITIS

Osteoarthritis is a joint degenerative disease that affects about 50% of all people above the age of 60 in North America. It is associated with a thinning and local loss of articular cartilage from the joint surfaces, osteophyte formations at the joint margins, swelling of the joint, and pain. The causes for osteoarthritis are not known, but risk factors include age, injury, and obesity. Osteoarthritis is often combined with a loss of muscle mass and movement control, and a decrease in strength.

It is well accepted that physiological loading of articular cartilage is essential for its health and integrity. Animal models of joint disruption through strategic cutting of ligaments or removal of menisci from knees have caused joint degeneration, presumably because of the altered loading conditions of the articular surfaces, although this is difficult to quantify in vivo. For example, when cutting the anterior cruciate ligament of the knee in a dog, cat, or rabbit unilaterally, there is an unloading of the experimental and an over-loading of the contralateral side that lasts for a few weeks (Figure 2.4.9). This intervention is associated with an instability of the knee, osteophyte formation at the joint margins, thickening of the medial aspect of the joint capsule and the medial collateral ligament, and increased thickness, water content, and softness of the articular cartilage (Herzog et al., 1993; Herzog et al., 1998). In the long-term, anterior cruciate ligament transection in the dog and cat have been shown to lead to bona fide osteoarthritis, as evidenced by full thickness loss of articular cartilage in some load bearing regions of the joint, leading to an increase in joint friction, decreased range of motion, pain, and a loss of muscle mass and strength in muscles crossing the knee (Brandt et al., 1991b; Brandt et al., 1991a; Longino et al., 2005; Clark et al., 2005).

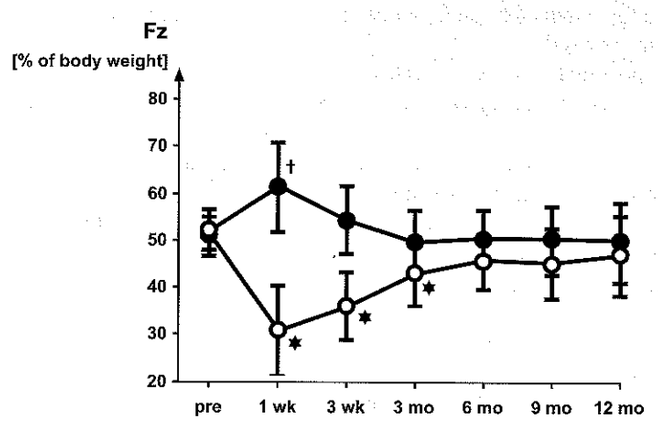

Figure 2.4.9 **Vertical ground reaction forces, Fz, normalized to body weight, as a function of time following unilateral anterior cruciate ligament (ACL) transection in cats (n = 7). Pre indicates testing before ACL transection, 1 wk, 3wk, ..., 12 mo indicate 1 week, 3 weeks, ...12 months post ACL transection. The vertical ground reaction forces are significantly (*) decreased in the ACL-transected (open symbols) compared to the contralateral (closed symbols) hind limb for 3 months post ACL transection. Thereafter, the differences are not statistically significant. One week following ACL transection, the vertical ground reaction force in the contralateral leg is greater (†) than in the pre-transection condition.**

Contact pressure measurements in intact cat patellofemoral joint that were loaded by muscular contraction showed that for a given amount of force transmitted through the joint, contact areas increased and peak contact pressures decreased by 50% in joints with early osteoarthritis compared to normal controls (Herzog et al., 1998). These results can be explained readily with the increased cartilage thickness and decreased stiffness observed in this phase of cartilage degeneration. Theoretical models with the altered geometries and functional properties have confirmed the experimental results. In late osteoarthritis, articular cartilage becomes thinner and harder than normal, and forces are transmitted across a decreased contact area and with peak pressures that are increased compared to the normal joint (Federico et al., 2004c)

It has been demonstrated that loading of articular cartilage affects the biological response of chondrocytes, which in turn affects the health and integrity of the cartilage matrix. The results are controversial, and there is no unified consensus on what loading is good or bad for cartilage health. However, it has been demonstrated that long, static loading is associated with an increase in cartilage matrix degrading enzymes, while intermittent physiological loading appears to strengthen the cartilage matrix through the formation of essential matrix proteins (e.g., Mow et al., 1994; Hasler et al., 1999.

One of the proposed pathways for transmitting load signals across the cell to the genome has been the cytoskeleton (specifically the integrin network). Integrins are transmembrane extra-cellular matrix receptors that have been shown to transmit forces from the matrix to the cytoskeleton of chondrocytes and vice versa. The mechanical signals transmitted by integrins may result in biochemical responses of the cell through force-dependent release of chemical second messengers, or by force-induced changes in cytoskeletal organization that activate gene transcription (Ingber, 1991; Ben-Ze'ev, 1991). However, a direct link between force transmission in integrins and a corresponding biosynthetic response has yet to be demonstrated.

Another potential cytoskeletal pathway for force transmission is actin. Guilak (1995) demonstrated that chondrocytes and their nuclei deformed when articular cartilage was loaded (15% compression) in an unconfined configuration. When the actin cytoskeleton was removed from the preparation and the same loading was applied to the cartilage, chondrocyte deformation remained the same, while nuclear deformation was changed, demonstrating an intimate connection between the actin cytoskeleton and cell nuclei. Although these results do not prove that actin works as a mechanical signalling pathway, they demonstrate that there are mechanical linkages that affect nuclear shape and might affect gene transcription.

A clinical observation in patients with osteoarthritis is that they often have diminished strength in the musculature surrounding the arthritic joint (Slemenda et al., 1997; Hurley, 1999; Slemenda et al., 1998), that maximal muscle contractions are not possible because of reflex inhibitions (e.g., Hurley & Newham, 1993), and that muscle contraction patterns change from normal for everyday movements (Herzog & Federico, 2005). Furthermore, it is generally accepted that muscles provide the primary loading of joints, with weight forces and external forces playing a relatively smaller role. Nevertheless, the role of muscles in the development and progression of osteoarthritis has largely been neglected, and some basic questions should be addressed in the future. These include the role of muscle activation patterns and muscle weakness as risk factors for osteoarthritis.

Only weak associations have been found between radiographic signs of joint disease and joint pain and disability in osteoarthritic patients (Claessens et al., 1990; McAlindon et al., 1993). Quadriceps weakness has been found to be one of the earliest and most common symptoms reported by patients with osteoarthritis (Fisher et al., 1991; Fisher et al., 1993; Fisher et al., 1997; Hurley & Newham, 1993). Furthermore, quadriceps weakness has been shown to be a better predictor of disability than radiographic changes or pain (Slemenda et al., 1997).

Therefore, there have been suggestions that muscle weakness might represent an independent risk factor for cartilage degeneration, joint disease, and osteoarthritis. Recent evidence from an animal model of muscle weakness supports this idea, showing that articular cartilage is degenerated following just four weeks of muscle weakness in knees that were otherwise not compromised (Figure 2.4.10). Based on the evidence that cartilage degeneration and osteoarthritis are associated with changed loading of joints, that mechanical loading influences the biosynthetic activity of chondrocytes, and that muscle coordination patterns and muscle strength are intimately associated with cartilage disease, conservative treatment modalities might represent promising approaches for preventing cartilage disease and osteoarthritis. These treatment modalities include appropriate movement biomechanics, exercise, and strengthening.

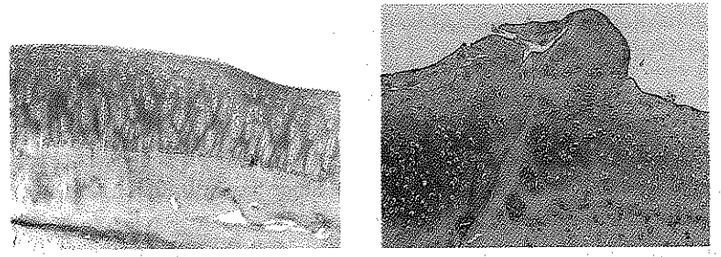

Figure 2.4.10 **Histological sections of articular cartilage from the femoral condyle of a normal and an experimental rabbit. The experimental rabbit received a single injection of botulinum toxin type-A into the knee extensor muscles causing weakness, and was sacrificed four weeks following the injection. The Mankin scores for the normal and experimental cartilage were 0 (normal) and 12 (signs of degeneration), indicating that muscle weakness may be a risk factor for joint degeneration.**

2.4.7 THEORETICAL AND NUMERICAL MODELS

Since it is virtually impossible at present to obtain in vivo joint mechanics (for example, instantaneous contact pressure distributions, or cartilage stresses and strains) much of our understanding of the local, internal joint biomechanics relies on joint contact and articular cartilage tissue models. These models have proven effective at estimating the contributions of fluid and matrix to the load sharing in the tissue, and describing stress-strain patterns in articular cartilage and chondrocytes with prescribed loading conditions. Selected cartilage modelling approaches are discussed below (Hasler et al., 1999; Federico et al., 2005; Her-

zog & Federico, 2005), ranging from single-phasic, homogeneous elastic models, to anisotropic, inhomogeneous, micro-structurally-based models of articular cartilage.

SINGLE PHASIC MODELS

The first theoretical models of articular cartilage were linearly elastic, homogeneous and isotropic. Hayes et al. (1972) related experimental data to the parameters of such models using results from indentation testing. Articular cartilage was represented as a linearly elastic material bonded to a rigid bone. A plane ended indenter was pressed with a force, P, into the tissue. Hayes et al. (1972) derived an equation for the shear modulus, μ, for this situation, assuming small strain theory and a frictionless indenter:

$$\mu = \frac{P(1-\nu)}{4aw\kappa(a/h, \nu)} \tag{2.4.1}$$

where:

ν = Poisson's ratio of the material
w = displacement imposed by the indenter
h = thickness of the cartilage layer
κ = scale factor depending on the aspect ratio a/h and the Poisson's ratio, ν

With this model, cartilage properties can be described by a single value for the elastic modulus, if a specific Poisson's ratio is assumed. Since the material is assumed to be elastic, its properties are independent of time. Therefore, creep and stress relaxation, inherent in articular cartilage, cannot be studied. An elastic model may be used for the study of instantaneous or equilibrium responses, when fluid flow is small or absent, and cartilage may behave almost like an elastic material. Both applications are confined to small loads to stay within the limits of the infinitesimal deformation assumption. Therefore, this approach is not appropriate for many physiological loading conditions.

In order to account for the experimentally observed creep and stress relaxation properties of cartilage, viscoelastic models have been proposed. The basis for viscoelastic models is the generalized Kelvin-Voigt-Maxwell spring-dashpot model (Figure 2.4.11). The linear springs produce instantaneous displacements proportional to the applied forces, while the dashpot produces velocities proportional to the applied forces. Using a viscoelastic model, Parsons and Black (1977) predicted the instantaneous and the long-term shear modulus for normal rabbit cartilage.

In summary, the use of single-phase models for the determination of the shear or Young's modulus requires that a specific Poisson's ratio for articular cartilage is assumed. It is not possible to separate the intrinsic cartilage properties associated with the solid matrix and fluid flow. Single-phase models are not suited for analysis of the internal mechanics of articular cartilage, or to estimate the loads acting on structural elements of cartilage. These models can merely provide an estimate of the external forces and the associated joint contact mechanics.

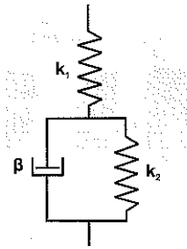

Figure 2.4.11 Scheme of the generalized Kelvin-Voigt-Maxwell spring-dashpot system.

BIPHASIC AND CONSOLIDATION MODELS

Interstitial fluid movement is thought to be the fundamental cause of the viscoelastic behaviour of articular cartilage. Thus, a structural model of articular cartilage should include at least two phases: a solid and a fluid phase. The behaviour of biphasic materials can be described in two ways

- A mixture theory, e.g., Fung (1993), that considers the material to be a continuum mixture of a deformable solid phase fully saturated by a fluid phase. At every point of the continuum, the two phases coexist, and the volumetric fraction fields obey the saturation condition, $\phi^s + \phi^f = 1$, at every point, where s indicates the solid phase, and f indicates the fluid phase.
- A consolidation approach (Oloyede & Broom, 1991), that considers the material to be a porous elastic solid saturated by a pore fluid that flows relative to the deforming solid.

Simon et al. (1996) proved that these two classes of models are equivalent if the fluid is assumed to be non-viscous.

BIPHASIC POROELASTIC MODELS

In biphasic models (Mow et al., 1980; Holmes & Mow, 1990), cartilage is represented as a mixture of a solid phase (collagen-PG matrix), which is assumed to be porous, homogeneous, isotropic, linearly elastic and with constant isotropic permeability, and a fluid phase (interstitial fluid), which is assumed to be non-viscous.

The solid and the fluid phases are assumed to be incompressible and immiscible. However, the mixture of an uncompressible solid and an uncompressible fluid can be globally compressible if fluid is allowed to escape through the boundaries of the system. Biphasic poroelastic models can explain the viscoelastic behaviour of cartilage in compression as the frictional drag associated with interstitial fluid flow. Movement of interstitial fluid determines the stress history for articular cartilage in confined compression (Figure 2.4.12). The stress rises with fluid exudation during compression because of the inherent resistance to fluid flow. During the relaxation phase, fluid redistribution decreases the stress in the compressed matrix. At equilibrium, the stress within the solid matrix represents the entire tissue stress.

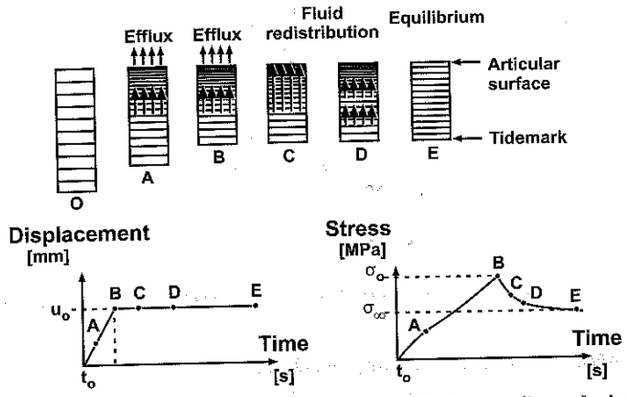

Figure 2.4.12 **Movement of the interstitial fluid in articular cartilage during a confined compression test, performed in displacement control. The displacement is applied with a linear ramp (A), and kept constant for the reminder of the test (B to E). The fluid starts to flow outwards as soon as the displacement is applied. The stress reaches its maximum value at the end of the displacement ramp (B). The fluid continues to flow, and this causes the stress to relax and tend asymptotically to the equilibrium value (E), which is reached when the fluid flow has ceased. From Mow and Rosenwasser; reproduced with permission from the American Academy of Orthopedic Surgeons.**

According to the biphasic constitutive law, the total Cauchy stress, σ, acting on the tissue is the sum of the stresses acting on the solid (superscript s) and fluid (superscript f) phases:

$$\sigma = \sigma^s + \sigma^f \tag{2.4.2}$$

The stress in the solid phase is expressed as the sum of the purely elastic stress, σ^{el}, plus a portion of the fluid pressure, p, proportional to the solid volumetric fraction, ϕ^s:

$$\sigma^s = -\phi^s pI + \sigma^{el} \tag{2.4.3}$$

where:

I = identity tensor

The reminder of the fluid pressure (proportional to the fluid volumetric fraction, $\phi^f = 1 - \phi^s$) represents the stress in the fluid phase:

$$\sigma^f = -\phi^f pI \tag{2.4.4}$$

In this way, the total stress (2.4.2) can be expressed as:

$$\sigma = -pI + \sigma^{el} \tag{2.4.5}$$

By defining the effective filtration velocity as $w = \phi^f(v^f - v^s)$, Darcy's law, describing the filtration of the fluid phase within the solid phase, reads:

$$w = -k \text{ grad } p \tag{2.4.6}$$

As the solid and the fluid phase are *intrinsically* incompressible, the continuity equation can be written in terms of volumetric fractions rather than mass densities (v^s is the velocity field in the solid phase, and v^f is the velocity field in the fluid phase):

$$\text{div}(\phi^s v^s + \phi^f v^f) = 0 \tag{2.4.7}$$

Euler's equation for the whole system is written assuming negligible inertial effects, i.e., negligible acceleration, and negligible external volume forces:

$$\underset{\approx 0}{\cancel{\rho f}} + \text{div}\sigma = \underset{\approx 0}{\cancel{\rho a}} \Rightarrow \text{div}\sigma = 0 \tag{2.4.8}$$

However, Euler's equation for each of the two phases must take into account the frictional drag force (per unit volume) $\phi^f w/k$, that the fluid phase exerts on the solid phase, which is accounted for with the minus sign in the equilibrium equation for the solid phase:

$$\text{div}\sigma^s = -\phi^f w/k \tag{2.4.9}$$

$$\text{div}\sigma^f = \phi^f w/k$$

Summing the two equations in (Equation 2.4.9) retrieves Euler's equation for the whole system (Equation 2.4.8):

$$\text{div}\sigma = \text{div}(\sigma^s + \sigma^f) = -\phi^f w/k + \phi^f w/k = 0 \tag{2.4.10}$$

In the linear biphasic model (Mow et al., 1980), the permeability, k, is assumed to be a constant, so that Darcy's law (2.4.6) is linear, and the constitutive equation for the purely elastic stress, which features in Equations (2.4.3) and (2.4.5), is linear and isotropic:

$$\sigma_{ij}^{el} = \lambda \varepsilon_{kk} \delta_{ij} + 2\mu \varepsilon_{ij} \tag{2.4.11}$$

where:

ε = Green strain tensor for the solid phase

λ and μ = first and second Lamé's coefficients for the solid phase

Mow et al. (1980) applied the linear biphasic formulation to determine simultaneously the aggregate modulus, H_A, and Poisson's ratio, ν, of the solid phase, and the permeability, k, from a single indentation experiment. At equilibrium, interstitial fluid flow ceases and the entire load applied to the articular cartilage is carried by the solid phase, and the biphasic result reduces to the elastic solution found by Hayes et al. (1972). For indentation experiments, the fit between the theoretical solution and experimental data was poor for the early time response of creep. Mow et al. (1980) assumed that the poor fit was associated with the assumptions made to derive the biphasic indentation creep solution, which included negli-

gible inertial effects, negligible intrinsic viscoelasticity of the solid phase, frictionless porous-permeable indenter tip, constant cartilage permeability, and isotropic and homogeneous tissue.

The non-linear model of Holmes and Mow (1990) includes a non-linear, hyperelastic constitutive law, and a strain-dependent permeability that can better represent the physiological behaviour of articular cartilage.

The purely elastic stress is obtained by derivation of the strain energy density, U, with respect to the components of the right Cauchy stretch tensor in the solid phase, C:

$$\sigma_{ij}^{el} = \frac{2}{J} F_{ik}\left[\frac{\partial U}{\partial C_{kl}}(C)\right]F_{jl} \tag{2.4.12}$$

where:

F = deformation gradient in the solid phase
J = determinant of F: J = det(F)

Holmes and Mow (1990) considered the material as isotropic. Therefore, the strain energy density function can be reduced to a function of the three principal invariants I_1, I_2, I_3 of the right Cauchy stretch tensor of the solid phase, C:

$$U(C) = W(I_1, I_2, I_3) \tag{2.4.13}$$

The strain energy given by Holmes and Mow (1990) is:

$$W(I_1, I_2, I_3) = \alpha_0 \exp[\alpha_1(I_1 - 3) + \alpha_2(I_2 - 3) - \beta \ln(I_3)] \tag{2.4.14}$$

where the coefficients α_0 (dimensions of energy per unit volume), α_1, α_2 (non-dimensional) are material parameters related to a material parameter β (non-dimensional) and to the homogenized values of the elastic Lamé's moduli for the solid phase, λ and μ, through the following equations:

$$\lambda = 4\alpha_0\alpha_2 \tag{2.4.15}$$

$$\mu = 2\alpha_0(\alpha_1 + \alpha_2) \tag{2.4.16}$$

$$\beta = \alpha_1 + 2\alpha_2 \tag{2.4.17}$$

α_0, α_1, and α_2 are fixed once λ and μ are known from small strain tests, and a value for β is chosen. The material is stable if α_0 is strictly positive, and α_1 and α_2 are non-negative, with at least one non-zero.

In the formulation of Holmes and Mow (1990), permeability depends on the volume fractions ϕ^f, ϕ^s and the third invariant of the right Cauchy tensor $I_3 = J^2$ for the solid phase, which is a measure of the apparent volume change (apparent because the local change of volume fractions makes the apparent density of the homogenized mixture change):

$$k = k_0\left[\frac{\phi_0^s \phi^f}{\phi^s \phi_0^f}\right]^{\kappa} \exp\left[\frac{M}{2}(I_3 - 1)\right] \tag{2.4.18}$$

where κ and M are non-dimensional material parameters to be determined experimentally.

Wu and Herzog (2000) expressed permeability as a function of the void ratio $e = \phi^f/\phi^s$, to implement the strain-dependent permeability into the Finite Element software ABAQUS. By setting $\phi^f/\phi^s = e$, $\phi_0^f/\phi_0^s = e_0$, $\phi_0^s/\phi^s = J$, and using the saturation condition, $\phi^f/\phi^s = 1$, one obtains:

$$k = k_0\left[\frac{e}{e_0}\right]^{\kappa} \exp\left[\frac{M}{2}\left[\left(\frac{1+e}{1+e_0}\right)^2 - 1\right]\right] \tag{2.4.19}$$

Qualitatively, the dependence of permeability on void ratio is intuitive. If the void ratio, $e = \phi^f/\phi^s$, decreases, the volume fraction of fluid decreases. In a fully saturated solid, the volume fraction of the fluid phase equals the volume fraction of the pores, thus, if the volume fraction of the pores decreases, permeability decreases as well.

The linear biphasic theory by Mow et al. (1980) was extended by Mak (1986) to the biphasic poroviscoelastic theory (BPVE), in which the solid phase was assumed to be intrinsically viscoelastic. This model allowed for the description of flow-dependent and flow-independent viscoelasticity in articular cartilage. The BPVE model increases the role of the solid phase and the deep layers in supporting applied loads within articular cartilage. In the BPVE model, predictions for confined compression during the early loading stage are improved compared to the linear elastic biphasic model, in situations in which loading is applied relatively "fast". Contributions from the intrinsic viscoelasticity of the solid matrix have been suggested to increase as permeability increases, as is the case for osteoarthritic cartilage with a damaged or fibrillated surface zone. In this case, intrinsic viscoelasticity of the solid matrix may alter the load-carrying behaviour of the tissue.

CONSOLIDATION MODELS

Oloyede and Broom (1991) wondered if cartilage could be described as a water-filled porous engineering material that undergoes mechanical consolidation like soils and clays. They performed simultaneous measurements of hydrostatic pore pressure and creep strain of the cartilage matrix during static compression in a one-dimensional consolidation configuration.

An idealized mechanism of consolidation (Figure 2.4.13) shows that the fluid initially carries the applied load (Figure 2.4.13b). After a critical hydrostatic pressure has been reached, fluid flows out of the porous matrix. Stress is then progressively transferred to the solid component of the tissue and consolidation starts. The tissue reaches the steady-state deformation when the hydrostatic pore pressure has decayed to zero. In the consolidated matrix, the final load is entirely carried by the compressed solid phase. The stress-strain relationship of the solid component, and therefore matrix stiffness, was shown to be non-linear for articular cartilage during consolidation. In addition, matrix stiffness increased progressively from low to medium to high strain-rate regimes. At very high strain rates, the fluid was locked within the matrix, thus greatly increasing tissue stiffness. The authors

concluded that a model based on the consolidation theory conceptualizes cartilage on a phenomenological level without cumbersome assumptions in the analysis of the cartilage response to load.

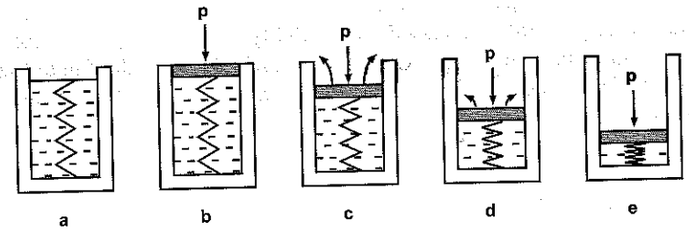

Figure 2.4.13 **Scheme of the consolidation mechanism: the spring represents the stiffness of the solid matrix, and the fluid represents the interstitial fluid (a). In a load control test, when the load P is applied to the porous punch (b), the fluid starts to flow outwards. Equilibrium (e) is reached when fluid flow has stopped, and the elastic force exerted by the spring equals the applied load, P.**

There is an equivalence of the biphasic and consolidation models for non-viscous fluids. As a result, consolidation models for non-viscous fluids can be applied to build finite element models to simulate problems with complex geometries and boundary conditions.

Van der Voet et al. (1992) modelled cartilage with poroelastic elements and compared their results with predictions obtained using the biphasic theory and results obtained experimentally. The authors concluded that, as predicted theoretically, results for cartilage compression from poroelastic models were comparable to those obtained using biphasic models. In the FE formulation of Suh and Bai (1998), the solid phase was considered viscoelastic, rather than elastic, as had been assumed in previous FE formulations. There are several other applications of the biphasic-poroelastic model to FE, which were used in a variety of problems of biomechanical interests. For example, Wu et al. (1999) and Wu and Herzog (2000) modelled the mechanics of chondrocytes embedded in the extracellular matrix, subjected to unconfined compression testing.

MULTIPHASIC MODELS

The main limitation of biphasic models is the impossibility to describe the structural elements that are responsible for the charged nature of articular cartilage, and to explain the origin of the physicochemical or electrochemical behaviour of the tissue, or both. Some constitutive theories that go beyond these limits are briefly discussed in this section.

Electromechanical Theory

Electromechanical models combine the laws for linear electrokinetic transduction in ionized media with the principles of the linear biphasic theory (Frank & Grodzinsky, 1987). When cartilage is compressed, mechanical-to-electrical transduction occurs, resulting in measurable electrical potentials. Deformation of the hydrated extracellular matrix causes a flow of interstitial fluid and entrained ions relative to the fixed charge groups of the extracellular matrix. Fluid flow tends to separate the mobile ions from the fixed charge groups

on the proteoglycans, producing a local voltage gradient, or streaming potential, that is proportional to the local fluid velocity. Conversely, application of electrical current across the cartilage produces a current-generated stress.

Triphasic Theory

The triphasic theory is an extension of the biphasic theory, with the addition of a third phase, representing cations and anions (Lai et al., 1991). Triphasic models have a chemical expansion stress that can be computed from the physico-chemical activities in the matrix due to the mobile ions and the fixed, negatively charged proteoglycan aggregates. Gu et al. (1998) developed a generalized multiphasic model including 2 + n constituents (one charged solid phase, one non-charged fluid phase and n ion species) that enables analysis of the diffusion processes of different ion species. Adding ion species to the biphasic model has helped in reproducing selected experimental results. However, the model remains macroscopic (as it remains a continuum mechanics model), and is dissociated from the microscopic, molecular structure of articular cartilage.

A poroelastic transport-swelling (PETS) FE model was developed by Simon et al. (1996) to simulate the interaction between mechanical deformation, fluid flow, and transport of ions through the matrix. The PETS model was shown to be equivalent to the triphasic model (Lai et al., 1991), and it provides a basis for the analysis of transport and swelling in soft tissues.

MOLECULAR-BASED MODELS

Kovach (1996) proposed a structural model of articular cartilage that incorporates glycosaminoglycans which exert drag on the fluid phase. The collagen network and its bound water restrain fluid flow and the distribution of proteoglycans.

This model gives a theoretical explanation for why proteoglycans occupy a different volume in vivo compared to in vitro. The swelling pressure of the tissue is decomposed into two parts: a charge-independent component, caused primarily by the configurational entropy of the glycosaminoglycan chains, and a charge-dependent component, directly caused by the glycosaminoglycan charge. It has been suggested that the charge-dependent properties dominate the swelling pressure in articular cartilage. The time-dependent mechanical properties of cartilage may be explained in terms of friction between the structural components of the matrix and fluid.

ANISOTROPIC, INHOMOGENEOUS AND MICROSTRUCTURAL MODELS

All models described so far are characterized by the isotropy, i.e., invariance of properties for rotations, and homogeneity, e.g., invariance for translations, of the constitutive equations. However, it is well acknowledged that cartilage is anisotropic (e.g., Cohen et al., 1998; Bursac et al., 1999; Wang et al., 2003) and inhomogeneous, (e.g., Schinagl et al. 1997). Therefore, cartilage has sometimes been modelled as a transversely isotropic material, with the transverse plane assumed parallel to the articular surface, and the symmetry axis perpendicular to the articular surface. These models can account for the different elastic

behaviour of cartilage in the axial and transverse directions, which has been observed experimentally.

Conversely, anisotropy and inhomogeneity of articular cartilage may be retrieved, to a certain degree, by modelling the structural components thought important in load bearing and force transmission across the tissue. Cells in articular cartilage can be approximated by revolution ellipsoids. Their shape changes from elongated in the deep zone to spherical in the middle zone to flattened in the superficial zone. Similarly, collagen fibres have a characteristic alignment within articular cartilage. Collagen fibres are perpendicular to the tidemark in the deep zone, randomly oriented in the middle zone, and parallel to the surface in the superficial zone (Hedlund et al., 1993). This arrangement of cells and fibres (Figure 2.4.14a) accounts for some of the anisotropy of the tissue. Assuming that the fibres in the superficial zone are parallel to the surface with no preferential direction on the superficial plane, the tissue can be represented as transversely isotropic (Figure 2.4.14b).

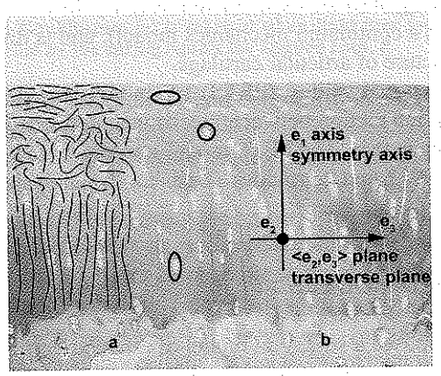

Figure 2.4.14 **Arrangement of the collagen fibres and cells in articular cartilage (a), and the consequent transverse isotropy (b).**

Farquhar et al. (1990) developed a fibril-reinforced micro-structural model of articular cartilage that accounts for the average effect of the collagen fibre network, but does not account for the spatial dependence of the arrangement of fibres. In the fibril-reinforced model of Li et al. (2000b), the depth-dependence of the mechanical properties of cartilage is taken into account, i.e., the model is inhomogeneous, and the collagen fibres are assumed to have tensile stiffness.

The models cited above do not account for the possible mechanical effects of cells on tissue properties. However, in small animals, cell volumetric concentration may exceed 20% (Clark et al., 2003), and, because their stiffness is much smaller than that of the surrounding matrix, they may affect the global elastic properties of the tissue (Federico et al., 2004b).

Based on a composite homogenization method (Walpole, 1981), Wu and Herzog (2002) built a microstructural three-layer model for the solid phase of the deep, middle, and superficial zone of articular cartilage, using zone-specific, structural arrangements of chondrocytes and collagen fibres. This model predicted the decrease of the axial elastic modulus

from the deep zone to the surface, but could only give a separate description of the three cartilage layers, and not a global solution for the entire tissue, as it is a straightforward application of Walpole's (1981) method for aligned inclusions. Walpole (1981) calculated the elastic tensor, L, for a N+1-phasic composite, with an isotropic matrix (index 0) and N transversely isotropic, spheroidal inclusion phases aligned with the e_1 direction:

$$L = \left[\sum_{r=0}^{N} c_r L_r A_r\right]\left[\sum_{r=0}^{N} c_r A_r\right]^{-1} = \left[\sum_{r=0}^{N} c_r Z_r\right]\left[\sum_{r=0}^{N} c_r A_r\right]^{-1} \quad (2.4.20)$$

where, for the r-th phase:

c_r = volumetric concentration ($\Sigma_{r=0}^{N} c_r = 1$)
L_r = elasticity tensor
A_r = strain-concentration tensor
Z_r = $L_r A_r$

Generalizing Walpole's (1981) method, a homogenization method in which the inclusions can take any orientation can be derived (Federico et al., 2004a). The N-th phase is assumed to have a statistical orientation, governed by the normalized probability distribution density ψ, which is a function of the direction. The set of all directions in space is represented by the north unit hemisphere S^{2+}, which is the set of all unit vectors w, lying in the positive hemi-space in the 1-direction. Vector w is conveniently represented as a function of the co-latitude angle, θ, and longitude angle, φ (Figure 2.4.15).

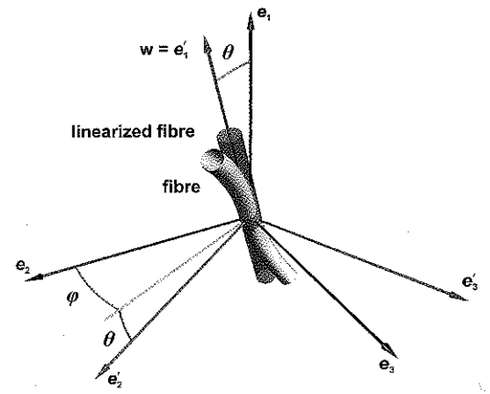

Figure 2.4.15 **Local reference frame for the representation of the direction, w, of the symmetry axis of an inclusion (a linearized fibre, in this example). The e'_1 axis of the local reference frame coincides with w, and its orientation with respect to the global reference frame (e_1, e_2, e_3) is given by the colatitude, θ, and the longitude, φ.**

With these assumptions on the N-th phase, Equation (2.4.20) can be generalized in the form:

$$L = \left[\sum_{r=0}^{N-1} c_r Z_r + \int_{S^{2+}} \psi c_N Z_N da\right]\left[\sum_{r=0}^{N-1} c_r A_r + \int_{S^{2+}} \psi c_N A_N da\right]^{-1} \quad (2.4.21)$$

where tensors Z_N and A_N are explicit functions of the direction w of the generic inclusion, and the surface integrals are performed on the unit hemisphere S^{2+}. By use of Walpole's (1981) formalism, tensors $Z_N(w)$ and $A_N(w)$ can be written as the linear combinations of Walpole's basis tensors B_α:

$$\begin{aligned} Z_N(w) &= \bar{Z}_N^\alpha B_\alpha(w) \\ A_N(w) &= \bar{A}_N^\alpha B_\alpha(w) \end{aligned} \quad (2.4.22)$$

where Walpole's components, $\bar{Z}_N^\alpha$ and $\bar{A}_N^\alpha$, *do not* depend on the direction, w (Federico et al., 2004a), as the dependence on w is accounted for by the basis tensors B_α. On the basis of these considerations, Equation (2.4.21), can be written as:

$$L = \left[\sum_{r=0}^{N-1} c_r Z_r + c_N \bar{Z}_N^\alpha \int_{S^{2+}} \psi B_\alpha da\right]\left[\sum_{r=0}^{N-1} c_r A_r + c_N \bar{A}_N^\alpha \int_{S^{2+}} \psi B_\alpha da\right]^{-1} \quad (2.4.23)$$

after factorizing the volumetric concentration, c_N, and Walpole's components, $\bar{Z}_N^\alpha$ and $\bar{A}_N^\alpha$. Equation (2.4.23) can be written in compact form, as:

$$L = \left[\sum_{r=0}^{N-1} c_r Z_r + c_N \bar{Z}_N^\alpha H_\alpha\right]\left[\sum_{r=0}^{N-1} c_r A_r + c_N \bar{A}_N^\alpha H_\alpha\right]^{-1} \quad (2.4.24)$$

where tensors H_α represent the directional average of the fourth order Walpole's (1981) basis tensors B_α:

$$H_\alpha = \int_{S^{2+}} \psi B_\alpha da \quad (2.4.25)$$

This method can be extended to inhomogeneous materials and adapted to cartilage by including the dependence of the various parameters featuring in Equation (2.4.21) on tissue depth. This inclusion of the various parameters in Equation (2.4.21) gave rise to a transversely isotropic, transversely homogeneous (TITH) model of articular cartilage (Federico et al., 2005). Transverse homogeneity is defined in analogy with transverse isotropy. While isotropy denotes symmetry, i.e., invariance, with respect to rotations of the reference frame, homogeneity denotes symmetry with respect to translations. Therefore, if transverse isotropy is the invariance for rotations with respect to a given direction (and orthogonal to a given plane), transverse homogeneity is the invariance for translations parallel to a given plane. In the TITH model, the cell volumetric concentration and aspect ratio, and the fibre volumetric concentration and spatial arrangement vary as a function of depth (transverse homogeneity, i.e., invariance under translations of the reference frame parallel to the transverse plane). If cells are described as revolution ellipsoids (having the symmetry axis parallel to the direction of depth), and fibres are given a statistical distribution of orientation (symmetric with respect to the direction of the depth), the resulting model is transversely isotropic, with the symmetry axis parallel to the direction of depth.

Because of the depth-dependence of the above mentioned parameters, the elastic modulus in Equation (2.4.10) is an explicit function of the normalized depth ξ ($\xi = x_1/h$, where h is the thickness of the cartilage layer), and it is calculated as:

$$\begin{aligned} L(\xi) = [&c_0(\xi)L_0 + c_c(\xi)Z_c(\xi) + c_f(\xi)\bar{Z}_f^\alpha H_\alpha(\xi)] \\ &[c_0(\xi)I + c_c(\xi)A_c(\xi) + c_f(\xi)\bar{A}_f^\alpha H_\alpha(\xi)]^{-1} \end{aligned} \quad (2.4.26)$$

where:

0 = matrix
c = cells
f = fibres

A transversely isotropic, transversely homogeneous model can predict the decrease in axial modulus from the tidemark to the surface, and can describe non-uniformities in the displacement fields. The prediction of the elastic moduli as a function of depth depends on the choice of the probability distribution, ψ. The mathematical form of the latter has been based on the assumption that the collagen fibres in articular cartilage are orthogonal to the tidemark in the deep zone, randomly oriented in the middle zone, and parallel to the surface in the superficial zone. With this assumption only, and not by suitably adjusting the various parameters featuring in Equation (2.4.26), the TITH model compared well with the experimental results of Schinagl et al. (1997) on the variation of the axial aggregate modulus with depth (Federico et al., 2005). Both the experimentally and numerically evaluated plots of the axial aggregate modulus, normalized to its value at the tidemark (Figure 2.4.16) show a high value at the tidemark, a plateau corresponding to the middle zone, and a small value at the surface, where the fibres are parallel to the surface and cannot bear axial load.

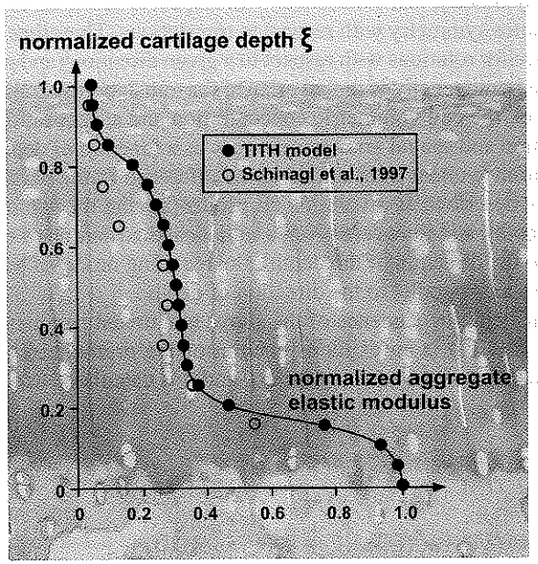

Figure 2.4.16 **Normalized aggregate elastic modulus (elastic modulus in uni-axial strain), as a function of the normalized cartilage depth, ξ, predicted by the TITH model, compared to the experiments performed by Schinagl et al. (1997).**

2.5 LIGAMENT

THORNTON, G.M.
FRANK, C.B.
SHRIVE, N.G.

2.5.1 MORPHOLOGY AND HISTOLOGY

MORPHOLOGY

The word ligament is derived from the Latin word *ligare*, which means "to bind". Ligaments consist of elastin and collagen fibres and attach one articulating bone to another across a joint. The major functions of ligaments are to:

- *Attach* articulating bones to one another across a joint,
- *Guide* joint movement,
- Maintain joint *congruency*, and
- Possibly act as a positional bend or strain *sensor* for the joint.

Collagen is the main protein present in ligaments. It is found chiefly in fibrillar form, and oriented between insertions to resist tensile forces. The hierarchical structure of the collagen in the ligament midsubstance includes fibres, fibrils, subfibrils, microfibrils, and tropocollagen (Figure 2.5.1). Tightly packed tropocollagen molecules, which are

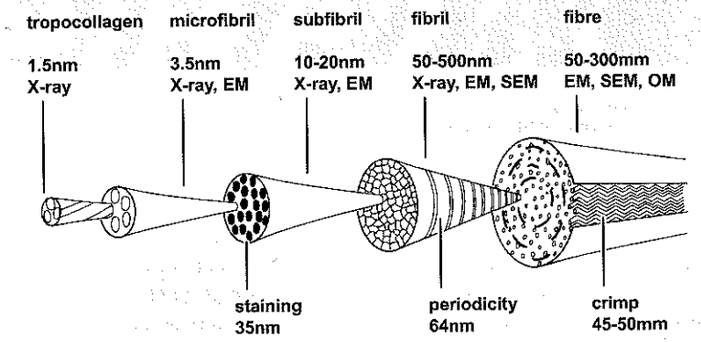

Figure 2.5.1 **Schematic illustration depicting the hierarchical structure of collagen in ligament midsubstance. EM = electron microscope; SEM = scanning EM; OM = optical microscope (from Kastelic et al., 1978, with permission of Gordon and Breach, Science Publishers Ltd.).**

approximately 1.5 nm in diameter, aggregate into groups of five, thereby becoming microfibrils of approximately 3.5 nm in diameter. The microfibrils group into subfibrils, which, in turn, aggregate to form fibrils. Fibrils are approximately 50 to 500 nm in diameter

with a periodicity (spacing) of 64 nm. Fibres are an aggregation of fibrils and are 50 to 300 μ in diameter. They are the smallest unit of the collagen hierarchy that can be seen under a light microscope. Fibres have an undulating crimp with a distance between amplitudes of about 50 μ. The crimp period can vary quite dramatically in different locations within the ligament. In the rabbit medial collateral ligament (MCL), fibroblasts tend to align in rows between fibre bundles and are elongated along the long axis in the direction of normal tensile stress (see Figure 2.5.2). Fibres and fibre bundles may or may not aggregate into fascicles (Figure 2.5.3). In the MCL, fascicles are not as obvious as they are in the anterior cruciate ligament (ACL).

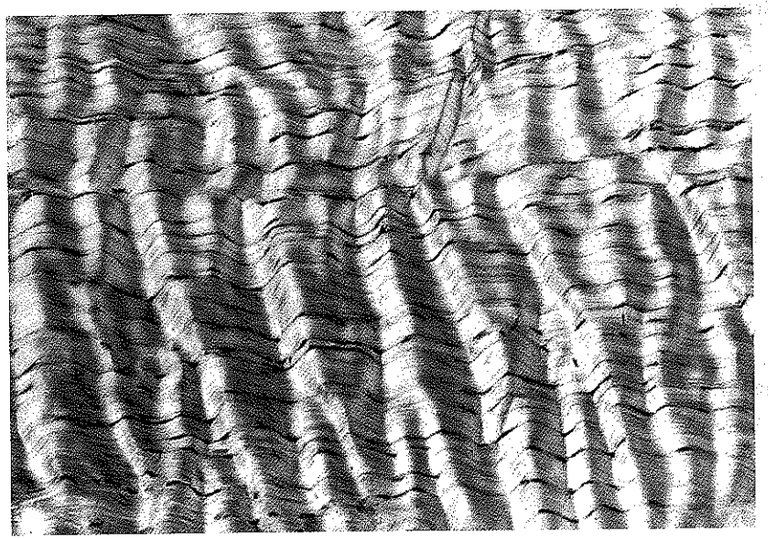

Figure 2.5.2 **Photograph illustrating crimped pattern of collagen in ligament. Fibroblasts may be seen interspersed between the collagen fibres.**

The surface of a ligament comprises a loose envelope known as the epiligament. Its collagen fibrils are of a smaller diameter than those of the midsubstance and are oriented in many directions. The epiligament contains a variety of cell types. These cells appear to have a greater proliferative ability than those of the midsubstance. Unlike the midsubstance, the epiligament encloses nerves and blood vessels that occasionally branch into the midsubstance. The function of the epiligament appears to be to:

- Protect the midsubstance of the ligament from abrasion,
- Support the neurovasculature,
- Control the water and metabolite flux, and
- Possibly act as a source for matrix, cells, and vasculature during maturation and healing.

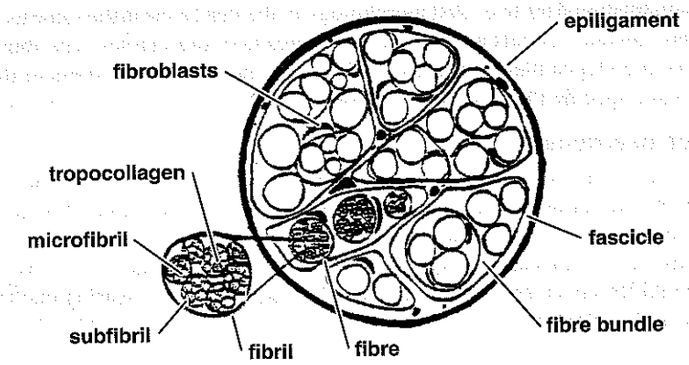

Figure 2.5.3 **Schematic diagram of a ligament in cross-section.**

Insertions

The structure of ligaments where they insert into bone is different from the midsubstance. Insertions anchor the ligament into the rigid, non-compliant bone. There are two general types of insertions: direct and indirect.

Direct insertions

Direct insertions, e.g., the femoral insertion of the MCL, occur where the ligament inserts directly into the bone. Direct insertions contain four different cellular zones, all of which occur within approximately 1 mm (Figure 2.5.4) of each other. The first zone is normal ligament midsubstance, with organized parallel collagen bundles, some elastin, and elongated fibroblasts. The second zone consists of non-mineralized fibrocartilage in which the cell numbers increase, become more ovoid, increase in size, and lie in rows. The collagen fibrils continue to extend into this region. The third zone may be characterized as min-

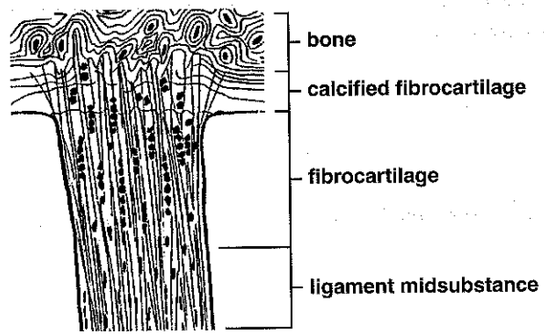

Figure 2.5.4 **Schematic diagram of a zonal ligament insertion into bone. The bone is at the top of the diagram, the ligament at the bottom (from Matyas, 1985, with permission).**

eralized cartilage and is clearly distinguishable from the previous zone by the *tidemark*, which is an undulating dark line. Cell morphology in the third zone is the same as in the second zone, but mineral crystals appear that are aggregated into masses. The fourth zone is where ligament collagen blends directly with bone collagen. The thickness of these zones is tissue and age specific (Matyas et al., 1990).

Indirect insertions

Indirect insertions occur where the ligament temporarily inserts into the periosteum during growth and development. The periosteum is, in turn, connected to bone. A typical example is the tibial insertion of the rabbit MCL (Matyas, 1990).

Insertions are mechanically stiffer near bone than near the ligament midsubstance. Such stiffening could lessen stress concentrations and reduce the risk of tearing due to shearing of the tissue at the interface.

Nerves

Recent years have seen much research into the role of the neural components of ligaments. As yet, the exact function of nerves in ligaments is not clear. It is speculated that they permit the sensing of joint position, the monitoring of ligament tension and integrity, and that they initiate protective reflexes. Some investigators have produced muscle activity by stimulating the nerves in ligaments (Sojka et al., 1989; Barrack & Skinner, 1990; Kraupse et al., 1992).

For the knee joint, two groups of nerves have been identified: one anterior and one posterior. These nerves respond to active and passive motion throughout the joint's range of motion. Their greatest responses occur at the extremes of knee motion, possibly warning of impending injury. Experimental stimulation of these receptors has been shown to cause reflex activation in the surrounding muscles (Adams, 1977; Kennedy et al., 1982).

Blood vessels

A fine network of blood vessels is in the epiligament of the MCL. A few vascular channels penetrate from the epiligament into the ligament substance and then course longitudinally between collagen fascicles. However, ligament insertions are poorly supplied with blood. The blood supply appears to nourish the fibroblasts, enabling them to remain metabolically active.

HISTOLOGY

The healthy ligament looks like a simple white band of homogeneous fibrous tissue, but it is actually highly complex and dynamic. It is composed of a few cells in a largely collagenous matrix.

Cells

Fibroblasts

Ligament cells are called fibroblasts or fibrocytes. Fibroblasts are not homogenous in ligament tissue and vary in size, shape, orientation, and number. Fibroblasts are usually

ovoid or spindle-like and are generally oriented longitudinally along the length of the ligament body. Both metabolic and histological experiments suggest that there may be fibroblast subtypes within the ligament, but these remain to be defined (Frank & Hart, 1990). Fibroblasts are responsible for synthesizing and degrading the ligament matrix in response to various stimuli. Presumably, fibroblasts prevent or repair ongoing microscopic damage. Therefore, despite their relative scarcity, fibroblasts are crucial to maintaining the status quo of ligaments.

Matrix

The matrix comprises virtually the entire body of the ligament. It consists of water, collagen, proteoglycans, fibronectin, elastin, actin, and a few other glycoproteins.

Water

Water makes up approximately two-thirds of the wet weight of a ligament. Water can be associated with other ligament components in a variety of ways. It can be structurally bound to other matrix components. It can be bound to polar side chains, be so-called transitional water (loosely bound), or be freely associated with the interfibrillar gel. Most water in ligaments is freely bound or transitional. Although the exact function of water in ligaments is unknown, it appears to be crucial for at least three main reasons. First, its interaction with the ground substance, particularly the proteoglycans, influences the tissue's viscoelastic behaviour (Amiel et al., 1990; Bray et al., 1991). Second, it seems to provide lubrication and facilitate inter-fascicular sliding (Amiel et al., 1990; Bray et al., 1991). Third, it carries nutrients to the fibroblasts and removes waste substances.

Collagen

Collagen comprises approximately 70-80% of the dry weight of ligament (Amiel et al., 1983; Frank et al., 1983a; Frank et al., 1983b). For more information about these collagen types, the reader should consult Miller and Gay (1992).

Type I:	The majority of ligament collagen is fibrillar, type I collagen.
Type III:	The second most common type is type III, which is also fibrillar.
Type VI:	The third most common is type VI, which is beaded filament.
Types V, XI, XII, and XIV:	Most ligaments also have small quantities of types V, XI, XII, and XIV collagen (the latter nearer insertions).

Collagen fibres within ligaments vary in size (diameter) from 10 to 1500 nm, a range that appears to be age-, tissue-, and species-specific (Parry et al., 1978a; Parry et al., 1978b; Frank et al., 1989; Yahia & Drouin, 1989). Fibre size may affect the strength of the material. Ligaments with larger bimodal collagen distributions tend to be stronger and able to sustain

higher stresses. Those with smaller unimodal diameters are more suited to resisting lower stresses. Collagen is enormously strong due to a combination of biochemical bonds known as molecular cross-links.

Proteoglycans

Ligament proteoglycans (mainly so-called small dermatan sulphate proteoglycans) comprise less than 1 percent of the dry weight of ligament, more than is found in tendon but considerably less than in cartilage (3 to 10 percent). The molecular structure of proteoglycans is described in Chapter 2.4. The role of proteoglycans in ligaments remains to be determined. However, ligaments (and tendons), because they experience primarily tensile forces, do not need the cushioning effect that proteoglycans give cartilage. Proteoglycans, with their pronounced hydrophilic properties, may instead be involved in regulating the amount and movement of water within the tissue. Therefore, proteoglycans would mainly influence the viscoelastic behaviour of the ligament.

Fibronectin

Fibronectin is a protein composed of two 220 kD subunits joined by a single disulfide bridge. This protein contains about 5 percent carbohydrate. In ligament, as in tendon (see section 2.6.1), fibronectin is found in small quantities in the matrix, usually in association with several other matrix components and blood vessels. Fibronectin also interacts with portions of the cell surface that are known to attach to intracellular elements, possibly forming part of an important matrix-cell feedback mechanism.

Elastin

Elastin is an elastic substance found in very small amounts in most skeletal ligaments (approximately 1.5 percent) in fibular form. However, in elastic ligaments, e.g., ligamentum flavum elastin fibres are about twice as common as collagen fibres. When unstressed, the insoluble globular proteinaceous elastin molecule takes on a complex, coiled arrangement, probably maintained in part by lysine derived cross-links. Elastin stretches into a more ordered configuration when it is stressed, reverting to its globular form when unstressed again. This behaviour probably accounts for part of the tensile resistance in ligament tissue and some of its elastic recoverability. The role of elastin is probably related to recovering ligament length after stress is removed. Elastin probably protects collagen, at least at low strains

Interactions of these components

Interactions between the various components of the extracellular matrix have, until recently, received little attention. A recent study (Bray et al., 1990) revealed, through a combination of cationic stains and enzymatic digestion, a network of electron-dense seams that connect cells and subdivide the matrix into compartments. The seams contain microfilaments of type VI collagen (Bray et al., 1990; Bray et al., 1993), microfibrils, and chondroitin sulphate-containing proteoglycan granules (Figure 2.5.5). The granules are suspended on the microfilaments and spiralled through the seams. The discovery of seams in the extracellular matrix of ligaments has led to the speculation that seams influence the viscoelastic behaviour of ligaments. The proteoglycans attached to the microfilament network may provide functional divisions within the matrix. As well, because of the hydrophilic nature of proteoglycans, water bound within the seams may act as a lubricant, facilitating sliding between adjacent collagen fascicles. Therefore, the seams would be an integral part of a ligament's viscous element.

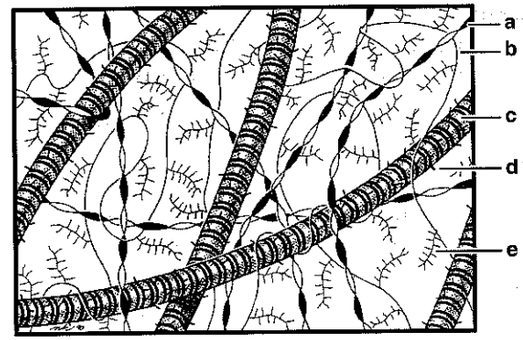

Figure 2.5.5 **Schematic diagram showing the proposed interrelationship between the elements of rabbit and human extracellular matrix. a = type VI collagen; b = non-beaded microfilaments; c = banded collagen fibrils; d = dermatan sulphate proteoglycan; e = chondroitin sulphate proteoglycan (from Bray et al., 1993, with permission).**

2.5.2 FUNCTION

The knee joint is used to illustrate ligament functions, because, like all weight-bearing joints, the knee is fundamentally concerned with stability over mobility. The four ligaments of the knee joint are illustrated in Figure 2.5.6. Their main passive restraining functions are summarized in Table 2.5.1.

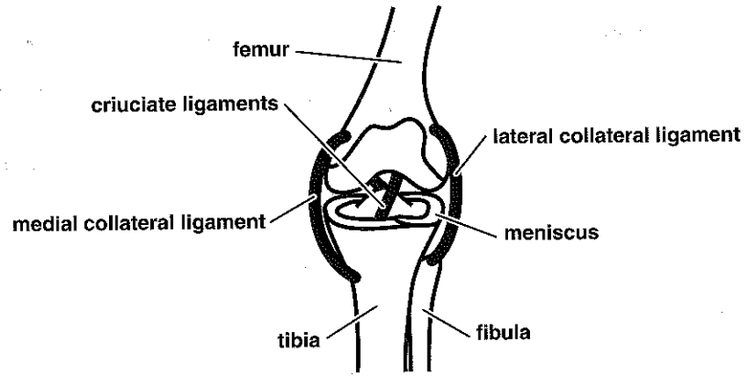

Figure 2.5.6 **Schematic diagram of the human knee joint from an anterior view. The cruciate (shaped like a cross) ligaments may be seen at the centre of the joint. The anterior cruciate ligament (ACL) attaches superiorly to the posterior lateral femoral condyle and inferiorly to the lateral anterior tibial spine. The posterior cruciate ligament (PCL) attaches superiorly to the medial femoral condyle and inferiorly to the posterior tibia. The collateral (parallel) ligaments lie lateral or to the side of the joint. The medial collateral ligament (MCL) is attached to the medial femoral condyle and the medial tibia, while the lateral collateral ligament (LCL) runs from the lateral epicondyle of the femur to the lateral fibular head.**

Table 2.5.1 Restraining functions of the four ligaments of the knee joint.

LIGAMENT	PRIMARY RESTRAINT	SECONDARY RESTRAINT	COMMENTS
ANTERIOR CRUCIATE LIGAMENT (ACL)	anterior tibial displacement	internal tibial rotation	no restraint to posterior tibial displacements
POSTERIOR CRUCIATE LIGAMENT (PCL)	posterior tibial displacement	external tibial rotation	no resistance to varus/valgus angulation
MEDIAL COLLATERAL LIGAMENT (MCL)	valgus angulation and external tibial rotation	anterior tibial displacement	
LATERAL COLLATERAL LIGAMENT (LCL)	varus angulation and internal tibial rotation	anterior and posterior tibial displacement	

The anatomical terms used in Table 2.5.1 are defined as follows:

Anterior: toward the front part.

Posterior: toward the back part.

Internal rotation: the frontal aspect of a body rotates toward the inside.

External rotation: the frontal aspect of a body rotates toward the outside.

Valgus: bent outward with respect to the proximal bone (for the knee, valgus means X-shaped) (Figure 2.5.7).

Varus: bent inward with respect to the proximal bone (for the knee, varus means O-shaped) (Figure 2.5.7).

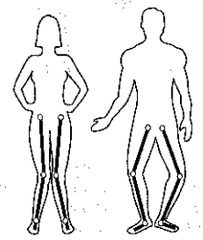

Figure 2.5.7 **Schematic illustration of valgus knees (knock-knees) on the left and varus knees (bow-legged) on the right.**

The knee joint has a complex ligament structure. In principle, the tibia has six possible degrees of freedom in relation to the femur (Figure 2.5.8): three translational (two sliding and one direct impingement and distraction) and three rotational. The ligaments, acting with the fibres of the joint capsule and the articular surfaces of the knee, restrict the range of motion, even when the muscles are completely relaxed.

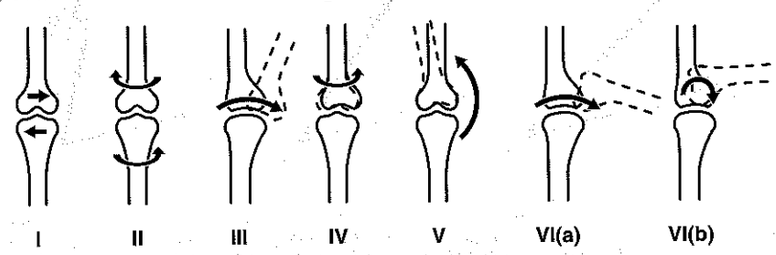

Figure 2.5.8 **Schematic diagrams illustrating the six possible degrees of freedom for the knee joint where (I) shows medial-lateral translation, (II) shows rotation, (III) shows anterior-posterior translation in the sagittal plane, (IV) shows tibial and femoral rotation, (V) shows varus-valgus rotation, and (VI) shows (a) the cruciate ligaments and (b) the collateral ligaments during flexion and extension in the sagittal plane.**

The joint may be flexed only through about 150°. The tibia can be rotated internally and externally relative to the femur through a range of about 35°. The range of varus and valgus movement is only about 5°. Only millimetres of translational movements parallel to the three axes are possible, and these are restricted by bone surface geometry and the ligaments. In normal physiological movements, however, it is rare for only one degree of freedom to be used. For example, knee flexion is associated primarily with rotation in the sagittal plane, but the tibia also translates along the frontal plane and rotates around the transverse plane while flexion occurs. Motions such as these are referred to as *coupled motions*. External loads seldom transmit only one component of force or moment across the joint. When examining the role of ligaments, however, we will simplify the possible combinations of the six degrees of motion.

CRUCIATE LIGAMENTS

Figure 2.5.9 shows a four bar linkage The tibial link AD and the femoral link CB are more or less parallel to the plateaux of the joints. The anterior cruciate AB and posterior cruciate CD are crossed (hence their name) and attach one condyle of one articulating bone to the opposite condyle of the apposing bone. Figure 2.5.9 shows how the shape of the four bar cruciate linkage changes during one particular degree of motion, flexion, and extension. Figure 2.5.9a shows the joint at full extension, (b) at 70° of flexion, and (c) at 140° of flexion. Between (a) and (c), the femoral link CB rotates 140° relative to the tibial link AD, and the cruciate links AB and CD rotate through 40° about their tibial attachments (A and D), and through 100° about their femoral attachments (B and C).

During this movement, the femoral condyles roll and slide on the tibia. The contact area moves backwards and outwards on the tibia in flexion, and forwards and inwards in extension. The femoral condyles diverge posteriorly and have reduced curvature. Thus, they sit in the menisci in an essentially anterior-posterior orientation in extension, but in flexion the diverging condyles force the menisci to assume a more medio-lateral curvature

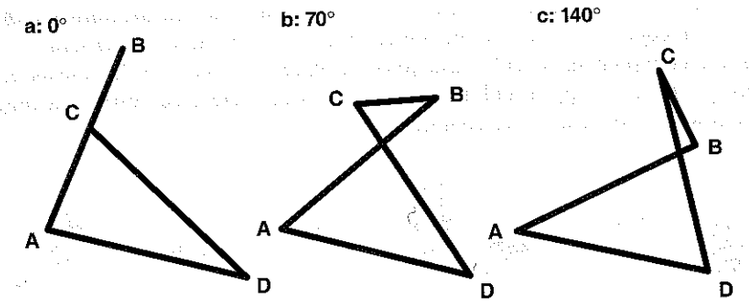

Figure 2.5.9 The cruciate four bar linkage ABCD at (a) full knee extension, (b) 70° of knee flexion, and (c) 140° of knee flexion. Between (a) and (c) the femoral link CB rotates through 140° relative to the tibial link AD, and the cruciate ligaments AB and CD rotate through 40° about their tibial attachments A and D, and through 100° about their femoral attachments B and C (from O'Connor et al., 1990, reprinted by permission of the Council of the Institution of Mechanical Engineers).

(Figure 2.5.10). It is through this mechanism that the condyles stay in contact with the menisci. The menisci are actually major load bearers in the knee, making the femur and tibia far more congruent than just a roller on a flat surface (Shrive et al., 1978). It takes about half

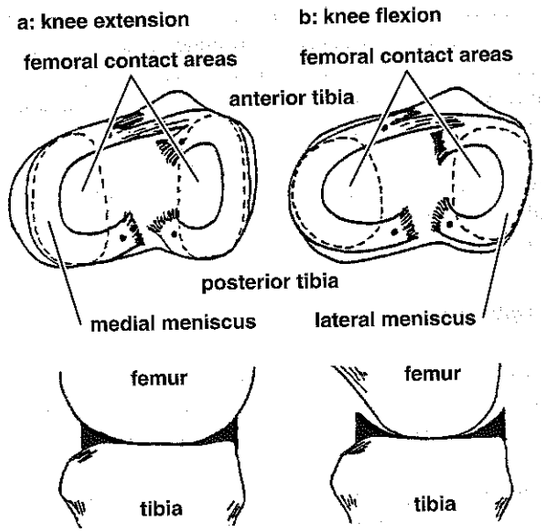

Figure 2.5.10 Schematic diagram of the knee joint showing distortion of the menisci during (a) extension and (b) flexion. When the menisci are viewed from above (top illustrations) the movement backwards and outwards from flexion to extension is apparent. The black dots show the points where each meniscus inserts firmly into the tibial eminence.

a body weight to make the femoral cartilage actually contact the tibial cartilage. At lower loads, typically all the load is carried by the menisci.

The cruciate ligaments play essential roles in controlling motion. The stresses that de-

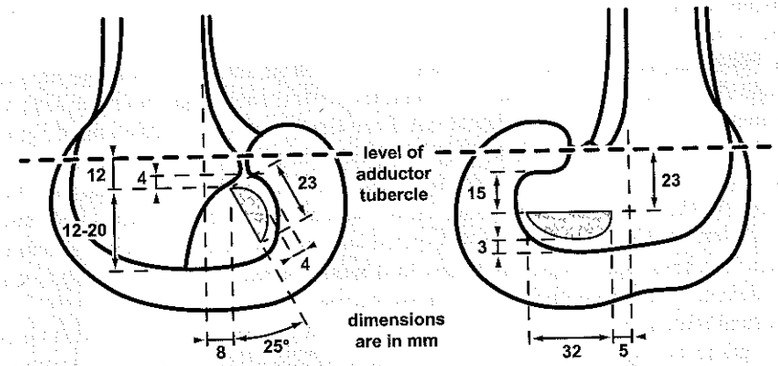

Figure 2.5.11 Average measurements and body relations of ACL (left) and the PCL (right) femoral attachment. The ACL attachment site is about 23 mm long and about half that wide. The PCL attachment site is about 32 mm in length and almost half that wide (from Girgis, 1975, with permission of J.P. Lippincott Co., Philadelphia, PA).

velop in the cruciate ligaments vary with joint angle. The twisted configuration of these ligaments and their wide insertion sites (Figure 2.5.11) appear well designed to deal with the varying load patterns.

Uniform stress is seldom achieved. The fact that the fibres are twisted suggests that the ACL is loaded in torsion as well as tension. The *screw home* mechanism as the knee comes

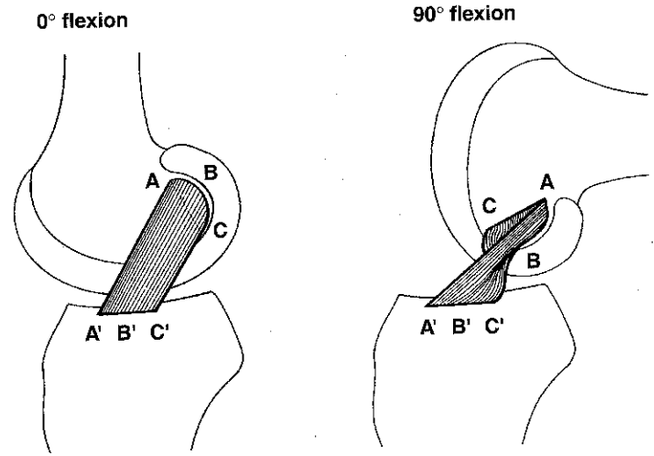

Figure 2.5.12 Schematic drawing of changes in shape and tension of ACL in extension (left) and flexion (right). The anteromedial band (A-A') lengthens and the posterolateral ligament aspect (C-C') shortens in flexion. Between (A-A') and (C-C') fascicles of an intermediate band (B-B') experience varying degrees of tension (from Arnoczky & Warren, 1988, with permission of J.P. Lippincott Co., Philadelphia, PA).

into extension, for example, involves a torsional rotation of the femur relative to the tibia. As the knee undergoes flexion and extension (and similarly internal, external, varus, and valgus rotations), the length and orientation of the fibres change (Figure 2.5.12). The broad

attachments to the femur and the tibia, combined with inter-fascicular sliding, allow various portions of the ligament to be relatively taut while others are lax, depending upon the knee motion. For example, in the ACL, the anterior fascicles are taut in flexion, but are relaxed to a certain degree in extension. The situation is the reverse for the posterior bundles; hence, the advantage of separate sliding fascicular fibre bundles and the variations of collagen crimp. The tension and relaxation in fibre bundles is clearly evident in cadaver specimens missing gravity and muscle loads. The implication is that, during normal activity, the pattern of tension and relaxation is the same. However, compressive forces can affect inter-insertional distances. The muscle forces associated with normal activity that initiate compressive loads in a joint may cause the bones to develop orientations to each other that are slightly different from those that occur in most cadaver tests.

In normal joint motion, together with the other ligaments and musculo-tendon units, the cruciate ligaments cope with varied angles of stress. The anterior cruciate ligaments are stronger in directions similar to their predominant fibre orientation than in directions aligned with the tibial axis (Woo et al., 1990). Figure 2.5.13 shows the force-deformation curves obtained during tensile testing of ACLs from young donors. The specimens loaded along the axis of the ACL demonstrate a steeper linear stiffness and higher ultimate load than those deformed along the tibial axis. These results indicate that the cruciate ligaments are favourably oriented to take up load in flexion and extension, and varus and valgus movements that approximate the ligament's angle of alignment. Restraint of these movements is considered to be the prime function of this ligament complex in the knee.

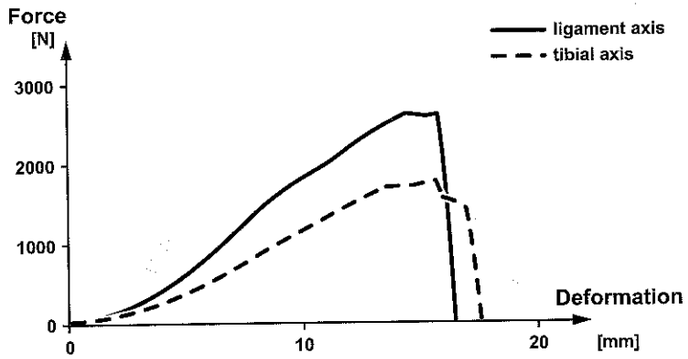

Figure 2.5.13 **Typical force-deformation curves for the femur-anterior cruciate ligament-tibia complex tested along the ACL axis (unbroken line) and along the tibial axis (broken line) (from Woo & Adams, 1990, with permission).**

COLLATERAL LIGAMENTS

The collateral ligaments are located outside the joint capsule (Figure 2.5.14), on the medial and lateral sides of the knee joint. Unlike the cruciate ligaments, the collateral

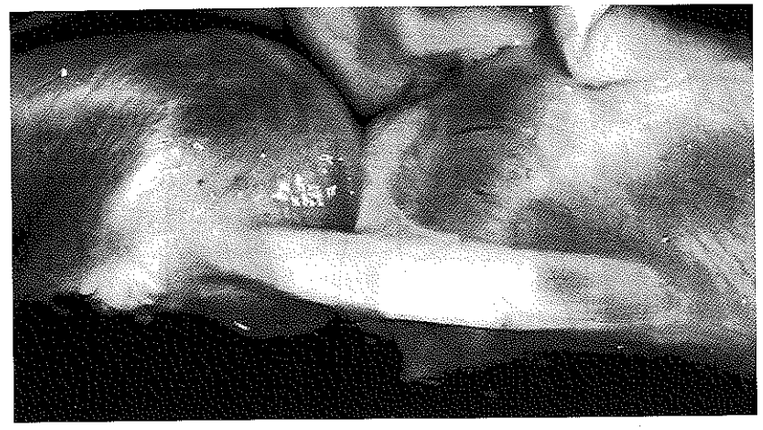

Figure 2.5.14 **Gross appearance of the rabbit MCL. The relatively parallel alignment of collagen fibres gives the MCL a cord-like appearance (from Bray et al., 1991, with permission).**

ligaments are not twisted. The main function of the collateral ligaments is to restrain varus and valgus angulation and rotation.

During varus angulation, the LCL takes up load, while the MCL relaxes. In valgus angulation, the roles of the collateral ligaments are reversed [Figure 2.5.8(V)]. During medial and lateral tibial rotation, the femoral condyles ride up the central eminence of the tibia, thus distracting the joint. The collateral ligaments resist the distraction, and consequently, the rotation. During rotation in the transverse plane, the collateral ligaments work together with the cruciate ligaments. During medial rotation, the MCL takes up a similar angulation to the ACL, and during lateral rotation, the LCL takes up a similar angulation to the PCL [Figure 2.5.8(IV)].

During flexion and extension, collateral ligaments play a secondary role to cruciate ligaments in restraining anterior and posterior displacement of femur and tibia, because alongside an increase in the joint angle during flexion, posterior bundles of the collaterals relax, while anterior bundles retain their length and take up some strain (Figure 2.5.15). This secondary role illustrates the advantage of sliding fascicles and the benefit of having different portions of ligaments able to take up stress at different joint angles.

2.5.3 PHYSICAL PROPERTIES AND MECHANICS

The tensile physical properties of all soft connective tissues can be classified into two general categories: structural and material. The structural properties of a ligament are derived from the behaviour of a bone-ligament-bone complex and thus involve the midsubstance of the ligament, the insertions, and the bone local to the insertions. The material properties describe the material irrespective of geometry. They are usually measured in the midsubstance of the ligament. In this section, both property types are discussed briefly as

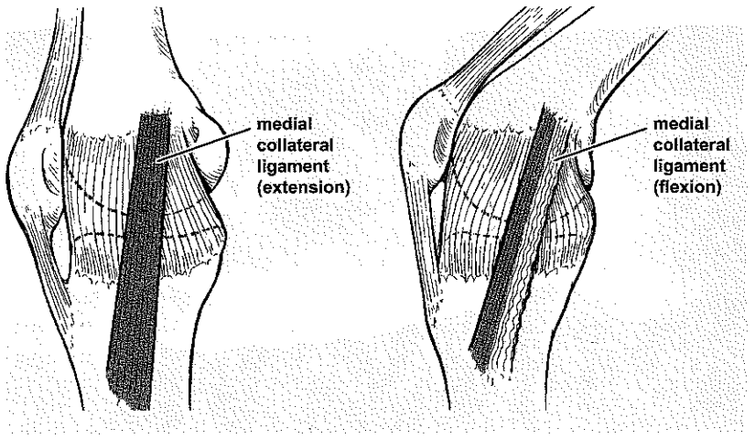

Figure 2.5.15 **The MCL at knee extension (left) and knee flexion (right). When the knee is fully extended, the fibres of the MCL are equally aligned and fully resist valgus angulation and tibial rotation. When the knee is in the flexed position, the anterior portion of the MCL remains taut while the posterior portion is relaxed. The anterior portion remains able to resist valgus and rotational stresses (from Indelicatio, 1988, with permission of Churchill Livingstone, New York).**

they pertain to the ligament model with which we have greatest experience, the rabbit MCL. Read the analogous section in Chapter 2.6 on tendon, as tendinous properties can be characterized similarly and are, at least in a gross sense, somewhat similar.

STRUCTURAL PROPERTIES

The non-linear force-deformation curve

Figure 2.5.16 shows a typical tensile force-deformation curve for ligaments. The stiffness (rate of change of force with deformation) of ligaments varies non-linearly with force. This non-linear behaviour allows ligaments to permit initial joint deformations with minimal resistance. The area under the curve in region I of Figure 2.5.16 is small compared, for example, to a straight-line relationship. Together with other ligaments, bone geometry and active muscles, ligaments work within their low-force range to guide bones through normal movement. At higher forces, ligaments become stiffer, thereby providing more resistance to increasing deformations. It is assumed that such stiffening protects the joint.

The non-linear force-deformation behaviour of ligaments occurs for at least two reasons: flattening out of collagen crimp and heterogeneous distribution of fibres. These reasons are described below.

Flattening out of collagen crimp

As described in more detail in Chapter 2.4, collagen (the main tensile-resisting substance in the ligament) is crimped. As with tendon, the crimp is thought to allow some extensibility of the ligament along its length under low forces. As tension is increased, the

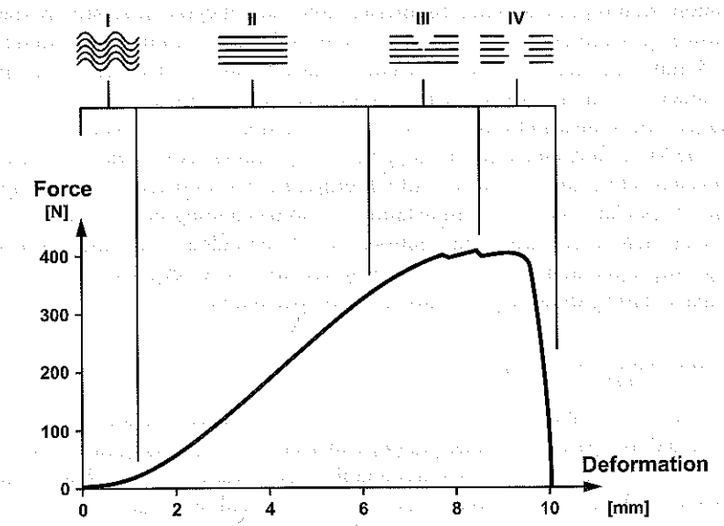

Figure 2.5.16 **A typical force-deformation curve for a typical rabbit ligament under monotonic loading. I = toe region; II = linear region; III = region of microfailure; IV = failure region. The top shows schematic representations of fibres going from crimped (I) through recruitment (II) to progressive failure (III and IV).**

crimp gradually flattens out. Once no more crimp can be removed, stiffness increases and an ever-increasing amount of force is required for further deformation. The toe region of the force-deformation curve (region I in Figure 2.5.16) is thought to correspond to the stretching out of crimp. With the crimp gone and the whole matrix under tension (the start of region II in Figure 2.5.16), a region with more constant linear stiffness (the linear region) begins.

Heterogeneous distribution of fibres

Neither fibres nor crimp are homogeneously distributed along the length of ligaments. As such, when ligaments are distracted, different fibres are recruited into load-bearing at different displacements. As noted above, when all the fibres have been recruited, the stiffness behaviour becomes more linear until some fibres (presumably those first recruited) fail. At this point, the net stiffness of the structure begins to drop, as shown in the fracture region of the force-deformation curve (region III in Figure 2.5.16). As some fibres fail, the load is redistributed onto the remaining fibres, increasing the load on them and the likelihood of their failure. It then takes little additional deformation to produce gross structural failure of the ligament through all the remaining fibres (region IV of Figure 2.5.16).

Microscopic examination shows some fibres crossing between parallel fibres in the ligament substance, some running perpendicular to the long axis and some at every angle between. While there are not many non-axial fibres (Liu et al., 1991) and they tend to be smaller than their longitudinally oriented partners, they should nonetheless contribute to non-linear stiffness behaviour as the ligament is loaded. Depending on how and where the non-axial fibres are connected, they could serve as tethers for longitudinal fibres. Alternatively,

the crossing fibres could be connected in a separate network from end-to-end in some oblique fashion. At this point in time, the microarchitecture of even the relatively simple MCL is not known. It is known, however, that gross midsubstance strains from around 8 percent (in up to 5 mm gauge lengths) are sufficient to cause failure of that area of the rabbit MCL (at least under certain in vitro boundary conditions (Lam, 1988)).

Collagen fibres must spiral from insertion to insertion as a joint rotates. For example, at the knee, the MCL fibres must spiral along their longitudinal axis as the joint flexes and extends. This has interesting implications to interpreting two-dimensional histology slices in any plane. It also has interesting implications in understanding how these spiraling fibres interact with each other during that motion. One is reminded of a dishcloth being wrung out, suggesting a potential mechanism from water flow or water expulsion from the interfibrillar space during spiralling, but this remains speculative.

Load relaxation and creep

Like other connective tissues, ligaments exhibit load relaxation and creep. When a ligament is pulled to a particular deformation, either once or repeatedly in cyclic succession, the load in a ligament decreases in a predictable way (Figure 2.5.17). This predictable decrease in load at fixed deformation is *load relaxation*. Load relaxation is a result of the viscous component of the ligament's response to load, and the most rapid part of the load decay occurs immediately after loading. Decay continues non-linearly until a steady-state value of load is achieved: this is the elastic component of the response. The relative proportions of the viscous and elastic components in any one force depend on the rate of load application and the previous load history as well as in a variety of test-specific parameters, e.g., temperature and the solution in which the test is carried out. The faster a load is applied, the less time there is for the viscous component to dissipate. A ligament will appear stronger and slightly stiffer under rapid versus slow load application.

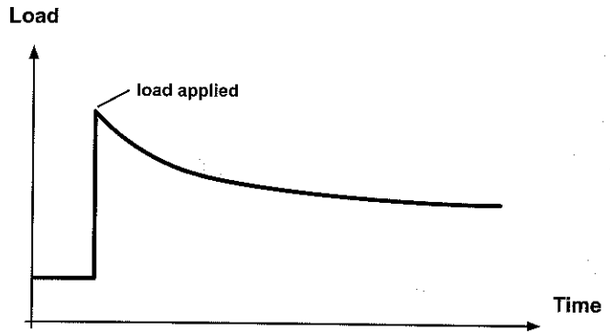

Figure 2.5.17 **Schematic load-relaxation curve for ligament.**

Creep is the analogous behaviour of a ligament under a fixed load when the load is either held or reached repetitively in a cyclic fashion. Creep is the increase in length over time

under a constant load. With creep, as with load relaxation, manifestation of the viscous component through time-dependent load or deformation changes eventually ceases (Figure 2.5.18).

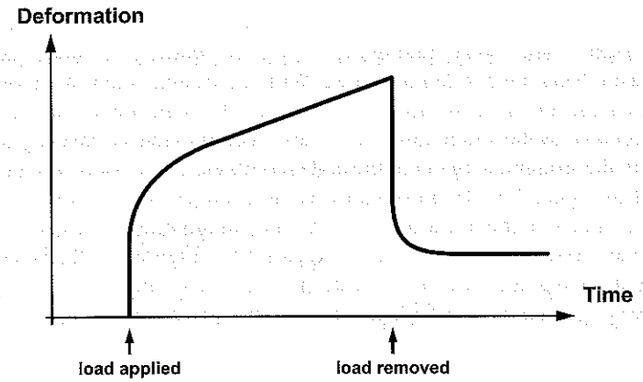

Figure 2.5.18 **Schematic creep curve for ligament.**

During cyclic load application, however, some of the viscous component can be recovered in each cycle (Figure 2.5.19). When the ligament is unloaded, the viscous component, while never recovering completely (at least during in vitro tests), can recover to over 90 percent of its original state after many hours in a relaxed condition. This recovery probably involves some combination of water influx, returning collagen crimp, elastin tensile force, and decreasing collagenous organization under unloaded conditions.

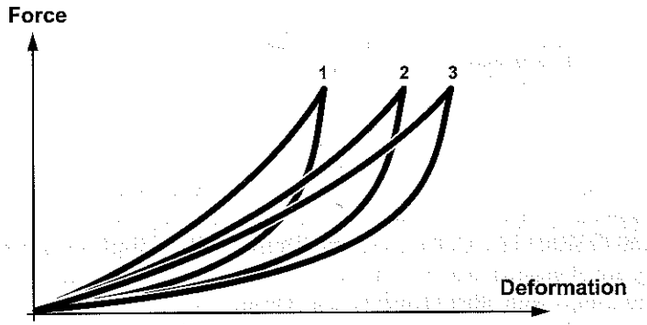

Figure 2.5.19 **Schematic force-deformation graph showing three successive cycles in displacement control to an upper load limit and a lower displacement limit, illustrating the viscoelastic creep effect of cycling upon a ligament.**

MATERIAL PROPERTIES

Non-linear behaviour

The material behaviour of ligaments, i.e., stress-strain behaviour, is also non-linear (Woo et al., 1982b; Lam, 1988), both under monotonic loading and under conditions in which viscoelastic behaviour is demonstrated. With increasing strain in a monotonic test, stress increases in the ligament, as shown in Figure 2.5.20. In the toe region (region I), there is little stress relative to the strain applied. As described previously, this region is thought to correspond to the straightening out of the collagen fibres. There follows a more linear region (region II in Figure 2.5.20), presumably as the collagen fibres take up load. A measurement of the tangent in the linear region is the tangent modulus which is often, but erroneously, called the elastic modulus. Finally, in region III of Figure 2.5.20, the curve flattens out, eventually dropping dramatically towards the strain axis. The flattening is presumably related to increasingly rapid microfailure, followed by catastrophic failure.

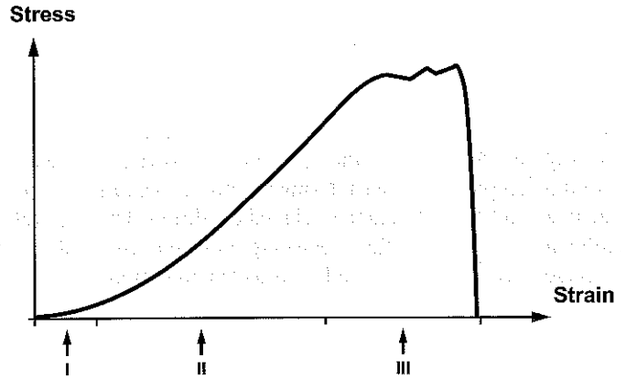

Figure 2.5.20 **Schematic stress-strain curve for ligament (I = toe region; II = linear region; III = failure region).**

The reasons for the non-linear behaviour at the stress-strain level are not as easy to explain as that of the structural behaviour, since less is known about the actual molecular nature of the ligament components or their interactions. Certainly, there must be some overlap with structural explanations. Collagen fibres themselves may display non-linear characteristics as they are elongated, due to a molecular rearrangement or some internal reordering of their relationships with other elements, e.g., elastin and fibronectin.

Water

Water makes up two-thirds of ligament composition which implies an important functional role. While these functions may be mainly biological, e.g., supply or removal of nutrients, water is known to contribute to the non-linear viscoelastic behaviour of the ligament in some significant way (Chimich et al., 1992; Thornton et al., 2001b). The amount of water

in the interfibrillar space may influence collagen stiffness, or the distances at which fibres can interact in a physical or biochemical sense. Further, because of its attraction to the highly negatively charged proteoglycan molecules, water may induce pressure gradients in the tissue that are further manipulated by movement.

PROBLEMS IN MEASURING PHYSICAL PROPERTIES OF LIGAMENTS

Measuring the physical properties of ligaments is not as simple as might be expected. Selected problems with these procedures are discussed in the following paragraphs.

Source of the tissue sample

The source of the tissue sample may have a considerable effect on the mechanical properties of the sample. All the properties of ligaments noted above are to some extent boundary condition specific. The boundary conditions include:

- Species,
- Type of ligament,
- Gender,
- Age,
- Activity,
- Drugs, and
- Diet.

Considering the boundary condition of age, for example, immature, mature, and aging tissue samples have different properties. As tissue matures, it strengthens due to increases in the size of collagen fibres and the number of molecular cross-links. Aging tissues, by contrast, experience a gradual, limited reversal of the maturation process. The in vivo load history of a tissue is another factor that vastly influences its properties. In vivo, inactivity results in a weaker tissue, while mobility and exercise increase tissue strength.

Because many boundary conditions may influence the mechanical properties of ligaments, consensus about the precise biomechanical behaviour of ligaments is lacking. As a result, we prefer not to publish either structural or material properties in this text that could be misinterpreted as absolute.

Different aspect ratios and trouble securing the ends of ligaments

Testing isolated ligaments is complicated by the different aspect ratios (length and width) of different ligaments and by difficulties in effectively securing the cut ends. Putting the free ends in clamps induces end-effects and often results in stress concentration at the grips, which damages the tissue and may contribute to premature failure or defective data. A bone-ligament-bone preparation provides more secure clamping, but increases the difficulty in separating the properties of the ligament midsubstance itself from those of the insertion sites. Special devices such as buckle transducers and magnetic field (Hall Effect)

displacement transducers have been used to estimate ligament forces during testing, but unfortunately they rely on direct contact with the tissue sample and may influence testing results. Measurements of ligament strains are also flawed. Optical analyzers that do not require contact with tissues have been used to quantify strains. However, the reported accuracy levels of these optical analyzers are known to be boundary condition specific (Lam et al., 1993), and the dye lines marked on the specimen may affect the strain being measured.

Measuring the cross-sectional area of a ligament

Measurements of stress have been compromised by the lack of an ideal method for measuring the cross-sectional area of a tissue sample. The irregular, complex shape and geometry of these tissues makes direct measurements difficult and errors large. Rigid calliper measurements, which are frequently used, require approximations, as the callipers are unable to take irregularities into consideration. Flexible callipers, which are better able to follow contours, are more accurate, but still require tissue contact. The only non-contact methods of measuring areas are optical, using either photography, or laser refraction to quantify distances. Laser refraction involves placing a specimen perpendicular to the path of a laser beam and rotating it by 180° or vice versa. The data of profile width and position are then recorded via a microprocessor. The centre of rotation and upper and lower boundaries are determined for each increment of rotation, and an iterative procedure is used to reconstruct the cross-sectional shape, from which the area may be calculated. Unfortunately, this technique misses depressions in an irregular surface. Like other techniques, this method is also unable to determine the circumference of the ligament with complete accuracy.

A *zero* strain position

The definition of a true *zero* strain position poses problems. The zero point on all the graphs used above is boundary-condition specific. The zero point depends on environment (including water content), load, and load history. The zero point is critical when properties are compared in absolute terms, i.e., at comparable forces and deformations, or comparable stresses and strains. A slight shift in the zero point of a test can drastically alter such comparisons (Figure 2.5.20). Changing water content by osmotic manipulation can affect this zero point (Thornton et al., 2001b). This has important implications for the need to control water content during in vitro tests, but also for in vivo length correction mechanisms in ligaments. Differences in environmental temperature can cause similar inaccuracies.

The necessity for well-documented biomechanical test procedures has been demonstrated. All the factors mentioned above must be taken into consideration before conclusions about ligament behaviour are drawn.

2.5.4 BIOLOGY AND FUNCTION

In vivo pressure recordings (used to estimate force) indicate that ligaments are exposed to repeated stress as part of daily activities (Holden et al., 1994). As such, ligaments are exposed to static and cyclic loading that causes creep. Examining the interplay between biology and function reveals potential mechanisms of creep in normal ligaments.

WATER

Water content plays a role in the viscoelastic behaviour of normal ligaments. In normal ligament, water flows out of the ligament during creep testing, resulting in a lower than normal water content at the end of the test (Thornton et al., 2000). The mechanisms driving this water exudation may involve a combination of fibre slack, Poisson's ratio, or osmotic pressure (Adeeb et al., 2004). If a period of *recovery* (unloading after loading) is permitted, water can flow back into the ligament to re-establish normal water content, but this process is stress- and time-dependent.

Decreasing the water content below normal values causes a decrease in relaxation and creep (Chimich et al., 1992; Thornton et al., 2001b). Correspondingly, an increase in water content above normal values causes an increase in relaxation and creep. Increasing the water content from normal creates a pre-stress in the ligament (Thornton et al., 2001b). Essentially, the functional length of the ligament decreases to accommodate the presence of greater than normal water content. The decrease in length is accompanied by an increase in cross-sectional area. These findings suggest that ligament viscoelastic behaviour could be affected by naturally occurring changes to water content in vivo, such as inflammation.

COLLAGEN

Despite similar responses to increased water content, relaxation and creep appear to be governed by different microstructural processes. When applying linear viscoelasticity within the linear framework of the quasi-linear viscoelastic theory (Fung, 1993), relaxation data were found to over-predict creep data for normal MCLs (Thornton et al., 1997). Fung (1993) speculated that creep is fundamentally more non-linear than relaxation, and the microstructural processes in a material undergoing creep could be quite different from relaxation.

The microstructural differences between creep and relaxation were investigated by recording the crimp pattern (marker of collagen fibre recruitment) at the beginning and end of relaxation and creep tests (Thornton et al., 2001a). Because relaxation is tested at a fixed deformation/strain, relaxation was found to be the behaviour of a distinct group of fibres recruited into load bearing at that fixed deformation with little or no change in the recruitment of fibres over the course of the test. Because creep is tested at a fixed load/stress and deformation is allowed to increase, creep was found to be the behaviour of fibres recruited initially and fibres recruited progressively over the course of the test.

The above observations were at stresses and strains in the toe region of the normal ligament stress-strain curve, thought to be within the normal, physiologic range. However, when ligaments are creep tested at stresses in the linear region of the stress-strain curve, the majority of the fibres are fully recruited (uncrimped) by the end of the test. Interestingly, the creep strains at the various toe region stresses were similar, despite doubling the stress. Yet, creep strain increased at a linear region stress. These findings indicate that fibre recruitment minimizes creep at toe region stresses, but this recruitment is limited at higher, linear region stresses.

A simple microstructural model demonstrated that the differences in creep and relaxation predictions could be accounted for by incorporating fibre recruitment (Thornton et al., 2001a). When the relaxation behaviour is taken to be that of fibres recruited into load-bearing, i.e. used to predict creep of recruited fibres, and coupled with progressive fibre recruitment, ligament creep behaviour is accurately predicted. The model also demonstrated that the load on the initially recruited fibres decreases as additional fibres are recruited into load-bearing.

This ability to redistribute stress is also demonstrated by the recovery of modulus following partial ligament failure (Thornton et al., 2002). In normal ligaments, modulus increases with successive loading cycles to toe region stresses. At a linear region stress, the ligament may have an increase in modulus for several cycles followed by an abrupt increase in strain with no corresponding increase in stress, i.e. a discontinuity, and a subsequent decrease in modulus. As the cyclic loading continues, the modulus increases, returning to the value achieved before the discontinuity. By evaluating the crimp pattern, the discontinuity was related to damage causing fibre rupture. Following fibre rupture, stress appears to be redistributed to the remaining intact fibres in order to avoid total ligament failure. From these results, different fibres in the ligament cross-section were at different stresses, with some stresses high enough to cause fibre rupture. Clearly, stress calculations based on total ligament cross-sectional area underestimate the stresses on the fibres that are recruited into load bearing.

Normal ligament mechanical behaviour is influenced by its most abundant component, water, and its major tensile load-bearing component, collagen. Examining the mechanical, morphological, and biochemical properties of ligaments healing from an injury further clarifies the importance of these and other components on ligament function.

2.5.5 FAILURE AND HEALING

Some of the most important factors that affect the normal integrity of ligaments include exercise, immobilization, aging and maturing, pregnancy, and injuries (see Chapter 2.8).

Accidental ligament ruptures in humans usually result from excessive loads. The rate of strain affects the type of ligament failure (Noyes et al., 1974). A study on primates revealed that there were only 29 percent ligamentous (or midsubstance) failures at a slow stretch rate, compared to 57 percent failures by tibial avulsion (insertion site at tibia). However, when the strain rate was increased a 100 fold, the percentage of ligament midsubstance tears increased to 66 percent and the percentage of tibial avulsions declined to 28 percent.

Ligaments that heal normally do so first by red blood cells and inflammatory white blood cells (disease preventing cells) entering the wound. Within days, a fragile fibrous scar composed mainly of blood-clot components and water appears in the wound. After about a week, metabolically active fibroblasts migrate into the wound to form an extracellular scar matrix. Eventually, these fibroblasts become the predominant cell type, as fluid and blood gradually dissipate.

When a ligament is injured and a gap is created between the torn ligament ends, the ligament heals with scar tissue that bridges that gap. This scar tissue is mechanically inferior to normal tissue, and several morphological and biochemical differences between normal and healing ligaments likely contribute to the inferior mechanical behaviour.

MECHANICAL

The failure properties of ligament scars are inferior to that of normal ligaments. Evaluating structural properties, MCL gap scars attain only 65 percent of the failure force of contralateral controls even after 40 weeks of healing (Chimich et al., 1991). Evaluating material properties (normalized for cross-sectional area), MCL gap scars achieve only 35 percent of the failure stress of controls at 40 weeks.

Like failure properties, viscoelastic properties improve with healing, but remain inferior to normal. Even after 14 weeks of healing, the creep strain of MCL scars is more than twice that of normal ligaments, when tested at the same stress (that corresponded to a physiologic stress in the toe region of the normal stress-strain curve) (Thornton et al., 2000). Also at 14 weeks, the modulus measured during cyclic loading of MCL scars is less than half of normal MCLs loaded to the same stress (Thornton et al., 2003).

MORPHOLOGICAL

The cross-sectional areas are larger for injured ligaments than for uninjured ligaments, even 40 weeks after the injury (Chimich et al., 1991). Because of this larger cross-sectional area, the failure properties of scar are worse when evaluated as a material property. The failure force was closer to that of normal, likely because of this larger cross-section of weak scar tissue.

Flaws (blood vessels, fat cells, hypercellular areas, and loose or disorganized matrix) account for a larger percentage of the area in MCL scar than in normal ligament (Shrive et al., 1995). The flaws decrease with healing, but remain greater than normal at 14 weeks. Stress concentrations arising from flaws likely affect both failure and viscoelastic properties.

Alignment of the scar collagen fibres along the longitudinal axis improves with healing and reaches normal values by 14 weeks (Frank et al., 1991). However, collagen fibril diameters are smaller than normal and do not change with healing by 40 weeks (Frank et al., 1992). Taking these collagen properties together, these small and initially poorly aligned fibres likely contribute to the mechanical inferiority.

BIOCHEMICAL

MCL scar water content is elevated early and decreases to normal values by 14 weeks (Thornton et al., 2000). Water content decreasing with healing may be related to the small improvement in viscoelastic behaviour over time, but cannot account for the persistent mechanical inferiority.

Proteoglycan (glycosaminoglycan) content of MCL scars decreases with healing, but remains elevated at 14 weeks (Frank et al., 1983a). This change in proteoglycan content may have altered the ratio of bound to free water and the resulting viscoelastic behaviour.

Collagen (hydroxyproline) concentration in MCL scars increases with healing and returns to normal values by 14 weeks (Frank et al., 1995). However, collagen (hydroxylysylpyridinoline) cross-link density increases with healing, but reaches about half of normal values at 14 and 40 weeks. Collagen fibres are small and initially poorly aligned, and never reestablish the same fibre interconnections as in normal ligament. These collagen properties as a whole likely contribute to both failure and viscoelastic inferiorities.

Remodelling occurs over many months or years. Scar flaws are removed, the number of collagen fibrils present increases, fibre alignment and cross-linking improves, and water and gylcosaminoglycan content decreases. However, there is no documented return to normal ligament.

2.6 TENDON/APONEUROSIS

HERZOG, W.

2.6.1 MORPHOLOGY AND HISTOLOGY

Tendon is a dense fibrous tissue that connects muscle to bone. Tendon is present in a wide variety of shapes and sizes, depending on the morphological, physiological, and mechanical characteristics of both the muscle and bone to which it is attached. Typically, tendon is glistening and pearly-white, and may take the shape of a thin cord or band, or a broad sheet. A variety of human tendons are well illustrated in Jozsa and Kannus (1997).

Usually, tendon consists of an external tendon, which is typically referred to as *tendon*, and an internal tendon, which is typically referred to as *aponeurosis*. The external tendon connects the muscle proper to bone. The aponeurosis provides the attachment area for the muscle fibres (Figure 2.6.1).

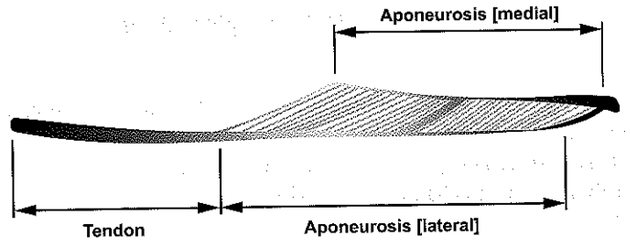

Figure 2.6.1 **Schematic illustration of a uni-pennate muscle with tendon and aponeuroses identified. The muscle is roughly based on the geometry of the cat medial gastrocnemius.**

A tendon may be constrained as it crosses a joint, either by bony prominences through which the tendon must pass or by specialized connective tissue sheaths, e.g., bicipital groove in the humerus and flexor retinaculum in the wrist. These constraints help to maintain the orientation of the tendon during joint motion. The retinacular sheaths are particularly important in the hands and feet, as tendons passing distally (towards the fingers or toes) over numerous small joints would be susceptible to injury if allowed to be displaced during finger or toe movements. A constrained finger flexor tendon is shown in Figure 2.6.2.

Despite the variable nature of tendon size and shape, every tendon has three distinct regions of organization: the muscle-tendon junction (myotendinous junction), the tendon *proper* (hereafter called tendon), and the bone-tendon junction (osteotendinous junction). Since the tendon region is often the most conspicuous region, it is the ideal place to begin a more detailed morphological and histological discussion.

Tendon is composed primarily of collagen fibres embedded in an aqueous gel-like ground substance. Since collagen comprises about 70 to 80% of the dry weight of tendon

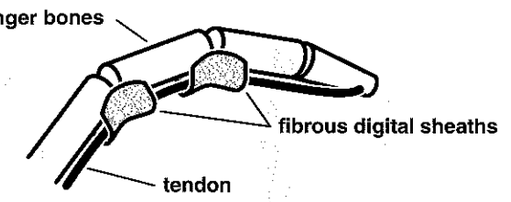

Figure 2.6.2 **Fibrous digital sheaths of the finger form a tunnel with the bone to keep the tendon close to the bone as the finger bends.**

(Elliot, 1965), a discussion of tendon morphology should first consider the biochemical organization of collagen.

Collagen is the main structural protein of animals. Although several different forms of collagen have been identified, e.g., type I collagen found in vertebrate tendon, collagen proteins are characterized, at least in part, by a predominance of the amino acids glycine, proline, hydroxyproline, and hydroxylysine. Hydroxyproline is unique to collagen.

The basic *unit* of collagen is tropocollagen, which consists of three non-coaxial helical polypeptide chains wound around each other to form a single closely-packed helix. The small glycine residues (a single proton), which occur approximately every third amino acid, allow for close packing between the three strands. The three strands are further stabilized by the hydrogen bonding from the relatively plentiful hydroxyproline residues. Each helical tropocollagen molecule is about 280 nm long. To make long strands of collagen fibres, tropocollagen molecules are covalently cross-linked to neighbouring tropocollagens at special amino acid sites where hydroxylysine is present. These amino acid sites give tropocollagen molecules the appearance of overlapping at approximately a quarter-length stagger. Five tropocollagen units in cross-section form the microfibril (Wainwright et al., 1982; O'Brien, 1992). The formation of a microfibril is schematically shown in Figure 2.6.3.

Microfibrils aggregate to form subfibrils. In cross-section, these subfibrils show 3.5 nm staining sites that correspond to the radii of the microfibrils. The subfibrils aggregate further to form fibrils. At this level of tendon organization, the electron microscope reveals a 64 nm longitudinal banding pattern. This banding pattern corresponds to the quarter-stagger overlap associated with the covalent cross-links between the tropocollagen units. Fibrils aggregate to form fibres and fibre bundles in which *crimping*, or longitudinal waviness of the collagen fibres, may first be apparent.

Fibre bundles aggregate to form fascicles. Fascicles are surrounded by endotenon, a connective tissue sheath composed of a well-ordered criss-cross pattern of collagen fibrils, proteoglycans, and elastin (Rowe, 1985). Endotenon contains the blood and lymphatic vessels, and nerves. Tendon cells, longitudinally-aligned among the fibre bundles, are visible at the fascicular level of tendon organization.

Fascicles aggregate into fascicle bundles and are surrounded by epitenon. Finally, several fascicular bundles are surrounded by paratenon, the outermost tendon sheath. Some tendons are enclosed by a further fluid-filled synovial sheath, which greatly reduces the friction associated with the movement of tendon against the surrounding tissue. A schematic diagram illustrating the structural hierarchy of tendon is shown in Figure 2.6.4.

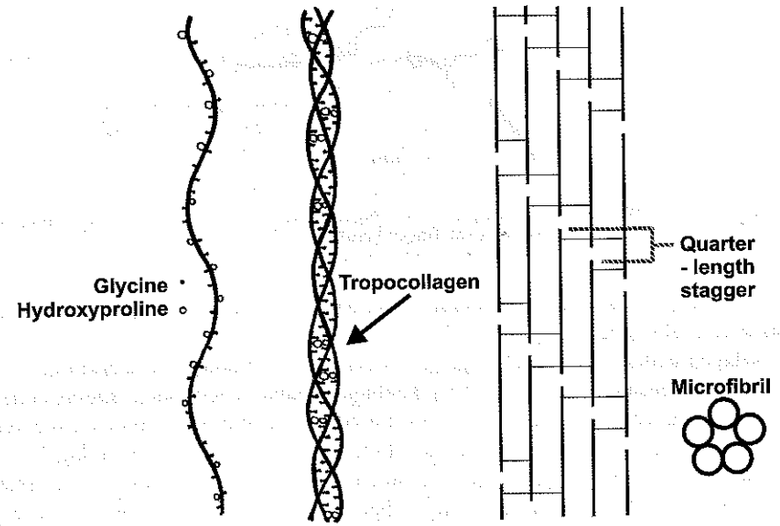

Figure 2.6.3 **Schematic diagram of tropocollagen and microfibril assembly.**

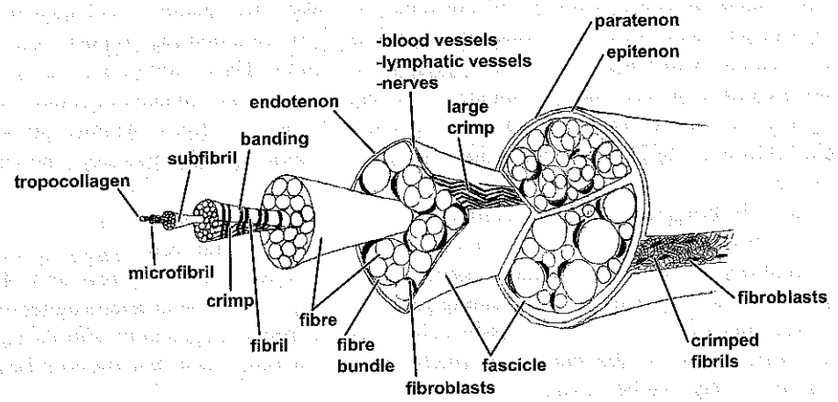

Figure 2.6.4 **The structural hierarchy of a tendon, from the tropocollagen molecule to the entire tendon. Connective tissue layers or sheaths envelop the collagen fascicles (endotenon), bundles of fascicles (epitenon), and the entire tendon (paratenon). Note that blood and lymphatic vessels and nerves are cut in the cross-section within the endotenon (from Kastelic et al., 1978, with permission).**

Golgi-tendon organs lie within the tendon and close to the myotendinous junction. Golgi-tendon organs are comprised of specialized nerve endings that lie in series with the contractile proteins of the muscle. Each golgi-tendon organ connects to the tendinous fascicles associated with approximately 10 muscle fibres, and sends a thick, myelinated afferent fibre to the spinal cord. The nerve endings extend many thin processes between the collagen fibres of their associated fascicles, partially encircling their associated fascicles. When the muscle contracts, tension is transferred to the tendon, causing the collagen fibres to compress the nerve endings and to initiate action potentials. As such, golgi-tendon organs are mechanoreceptors that monitor muscle tension. Afferent nerve fibres carry sensory information from the periphery to the spinal cord. The conduction velocities of the golgi afferents are enhanced by their relatively thick myelin and large size. Golgi-tendon afferents synapse with the internuncial neurons in the spinal cord and inhibit the alpha motor neurons of the corresponding muscle during isometric contraction. They may also excite the alpha motor neurons during cyclic movements, as has been shown for locomotion in the cat (Pearson, 1993).

The myotendinous junction is the region where the muscle joins with the tendon. Often, there is a myotendinous junction at both the origin and the insertion ends of the muscle belly. Transmission and scanning electron microscopy studies from a wide variety of vertebrate and invertebrate species show that the myotendinous junction is characterized by significant longitudinal surface folding (Figure 2.6.5). Several physical consequences are associated with this type of morphology, which greatly increases the area of contact between muscle and tendon (Tidball, 1991). The stresses transferred from the muscle to the tendon are greatly reduced in this region. The amplification in myotendinous contact area, calculated as the ratio between the myotendinous contact area and the physiological cross-sectional area of the muscle and its longitudinal end-folding area, has been estimated for several muscles, and appears to vary between 10- and 50-fold. Most of the values fall between 10- to 18-fold. Earlier studies by Trotter et al. (1985) suggested that the degree of infolding reflects the rate of tension development within the muscle, with slow twitch fibres having a larger junctional area than fast twitch fibres. However, more recent studies suggest that there is no consistent relationship between the amplification in myotendinous contact area and a physiological parameter, such as contractile speed or tonic versus phasic function (Trotter, 1993).

Figure 2.6.5 **The myotendinous junction (see arrows) as seen by transmission electron microscopy (from Jozsa & Kannus, 1997, with permission).**

Another consequence of the folded ultrastructure of the muscle-tendon junction is that the longitudinal folds facilitate the transfer of load by shear rather than by tension (Figure 2.6.6). The acute angle of contact between the muscle and tendon tissues ensures

that the shear component of loading is greater than the tensile component. For adhesive joints between engineering materials, it is desirable to maximize the shear component of loading and to minimize the tensile component because engineering adhesives are stronger in shear than in tension. Biological materials that constitute the mechanical junctions at the ends of muscle fibres may also be stronger in shear than in tension. However, no direct evidence for this statement is available (Trotter, 1993).

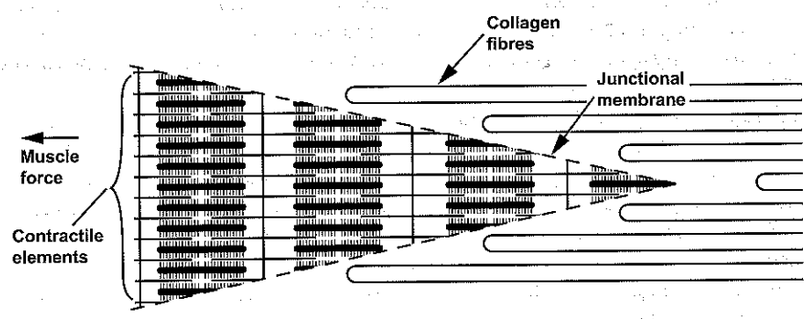

Figure 2.6.6 **Diagram of a myotendinous junction. Muscle force is applied parallel to the longitudinal axes of the myofilaments and the collagen fibres. The junctional membrane lies at an angle relative to the myofilaments. The acute angle with which the muscle and collagen fibrils meet creates a shear stress between the fibrils. If the fibrils met end-to-end, the junction would be loaded in tension.**

In vertebrate muscles, collagen fibres that form the areolar tissue of the endomysium (the muscle equivalent of the endotenon) become aligned near the muscle-tendon junction into a dense regular arrangement to form what Moore (1983) has termed a *microtendon*, which is one microtendon per muscle fibre. However, Ishikawa (1965) has pointed out that the collagen fibrils immediately associated with the fibre ends are not uniformly aligned with the fibre axis, but are more likely to have an isotropic arrangement, like those of the endomysium. The microtendon collagen fibrils, like those of the endomysium, have a uniform small diameter (Moore, 1983). At a short distance from the muscle-tendon junction, each microtendon blends with the tendon. The collagen fibrils of the tendon are heterogeneous in diameter, reaching much larger diameters than seen in the endomysium or microtendon. The microtendon thus forms a transitional structure for transmitting tension between muscle and tendon (Trotter, 1993).

The region where the tendon attaches to the bone, the osteotendinous junction, is morphologically distinct from both the tendon proper and the myotendinous junction. There are two types of attachment: one when the tendon becomes attached to epiphyseal bone and the other when the tendon approaches and attaches to bone at an acute angle.

When the tendon becomes attached to epiphyseal bone, the change takes place over four distinct, but well-blended, zones: fibrous tendon tissue; fibrocartilage tissue; calcified fibrocartilage tissue; and bone tissue. The transition from tendon to fibrocartilagenous tissue is characterized in part by a denser proteoglycan ground substance. Spindle-shaped

tendon cells gradually change into rounded cartilage chondrocytes. The chondrocytes and cartilage ground substance lie among the collagen bundles that continue from the tendon proper. Blood vessels are generally absent from the zone of fibrocartilage (Benjamin et al., 1986). The amount of fibrocartilage present in an osteotendinous junction varies widely among tendons, and between regions of the same insertion. This newly formed fibrocartilage merges with articular cartilage, where present (Benjamin et al., 1986). The zone of calcified fibrocartilage is evident by the presence of one or more basophilic lines or tidemarks (visible by light microscopy), indicating the transition between the non-calcified and the calcified fibrocartilage. The calcified fibrocartilage zone is adjacent to the bone (Figure 2.6.7). Chondrocytes are less numerous on the bony side of the tidemark.

When tendon approaches bone at an acute angle, the morphology of attachment appears to be somewhat different than that described for attachment to epiphyseal bone. In this case, the superficial collagen fibres of the tendon blend in with the periosteum that covers the bony surface. The deep collagen fibres of the tendon penetrate the periosteum, and attach directly into the bone.

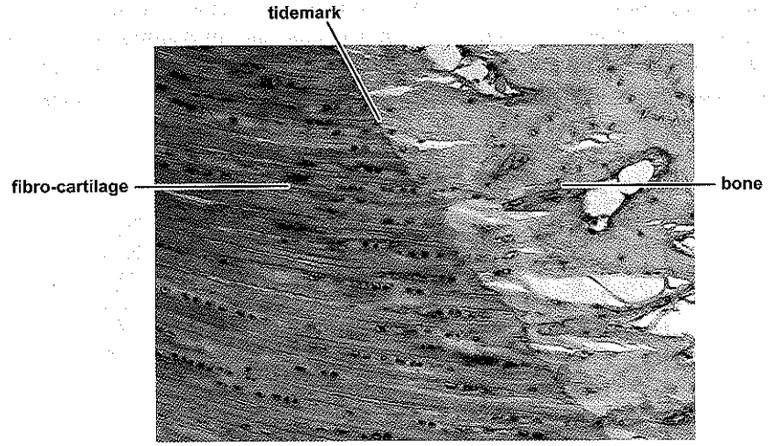

Figure 2.6.7 **Direct fibro-cartilagenous insertion into bone. The example shown is from a dog tendoachilles into the calcaneus (acknowledgement: Dr. J. R. Matyas).**

The functional significance of the epiphyseal-type of insertion is controversial. The gradual transition from fibrous tissue to bone may help to distribute forces over the attachment site, thereby, minimizing local stress concentration (Cooper & Misol, 1970; Noyes et al., 1974a; Woo et al., 1988). Benjamin et al. (1986) suggested that fibrocartilage is typical of epiphyseal attachments, because these tendons undergo a greater angular change during joint movement than do tendons inserting along the bony shafts.

2.6.2 PHYSICAL PROPERTIES

The primary role of tendon is to transmit the force of its associated muscle to bone. As such, tendon needs to be relatively stiff and strong in tension. Mechanical properties, such

as tensile stiffness and ultimate strength, are typically determined using conventional engineering testing machines where one end of the test specimen is fixed to an actuator and the other end is fixed to a load cell.

Mechanical testing of tendons has proven to be a challenge. The main difficulty is that specimens tend to slip out of the standard testing machine grips. Alternatively, if tendon specimens are tightly squeezed between gripping surfaces, stress concentrations occur at the grip-specimen interface, and often cause premature failure of the specimen at the grip. Recently, cryo-grips have been introduced. In cryogrips, the specimen is frozen at the location where it is gripped. Frozen tissue is stronger than fresh tissue, therefore, this technique largely eliminates the failure problem at the specimen-grip interface. Similarly, the air-dried ends of tendon specimens (the remainders of which were kept moist) provided strong gripping material for measurements of stiffness, hysteresis, and ultimate strength (Wang & Ker, 1995; Wang et al., 1995). Specimens can also be tested by gripping the bone at one end, and the muscle or tendon at the other end. If the material properties of the tendon proper are sought, the structural effects involving the insertion must be separated from the material effects. Ker (1981) discussed potential problems associated with measuring the mechanical properties of tendon, and suggested that problems can be minimized, for example, by using relatively long uniform tendons and measuring length changes, specifically, near the mid-region of the tendon with a lightweight length transducer that is attached directly to the tendon. Possibilities for gripping tendon are shown in Figure 2.6.8.

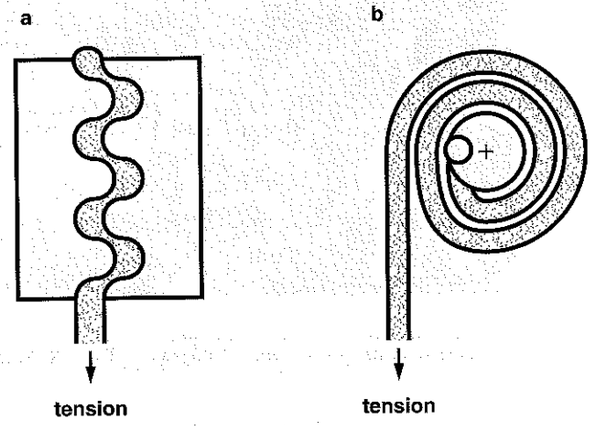

Figure 2.6.8 **Different grips for holding tendons. Serrated grips in (a) may have different shapes, but rely on friction between serration and specimen to help hold the specimen in place. Roller grips (b) are based on reducing the tension in the specimen as it is wrapped around the roller before the end is gripped.**

A typical stress-strain curve for tendon is shown in Figure 2.6.9. The curve illustrates the tensile response for a tendon specimen subjected to a single pull to failure. There are three distinct regions of the curve: toe, linear, and yield.

The toe region typically lies below 3% strain, a region in which specimen elongation is accompanied by very low stress. This low initial stiffness of tendon in the toe region is thought to be caused, in part, by the straightening of the collagen crimp. Rigby et al. (1959)

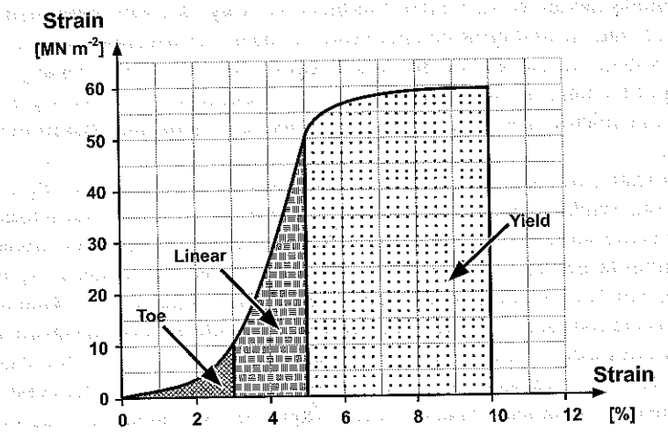

Figure 2.6.9 **Typical tendon stress-strain curve for a tensile test to rupture.**

studied rat tail tendon with polarized light and observed that the tendon lost its crimping pattern beyond strains of about 2 to 3%. However, Hooley and McCrum (1980) attributed the toe region to shearing action between the collagen fibrils and the ground substance of the tendon.

The linear region is evident beyond approximately 2 to 3% tensile strain. The slope of this linear portion of the curve has been used to define the Young's modulus of the tendon. This region of linear or *reversible* strain extends to about 4 to 5% (Wainwright et al., 1982). The Young's modulus for rat tail tendon is approximately 1.0 GPa (Rigby et al., 1959). The mean tangent moduli, derived from several aquatic and terrestrial mammalian species, ranges from 1.25 to 1.65 GPa with a mean across all species of 1.5 GPa (Bennett et al., 1986). Most of these measurements were obtained in dynamic tests at 1.0 to 2.2 Hz. Little variation in Young's modulus was found with frequencies in the range of 0.2 to 11 Hz.

Permanent deformation occurs beyond the region of linear or reversible strain. The ultimate or failure strain of tendon is about 8 to 10% (Rigby et al., 1959). There is a considerable yield region in which tendon deformation is accompanied by very little increase in stress. Tendon failure eventually results from collagen fibres pulling apart. The ultimate or failure stress of tendon is defined as tendon *strength*. The strength of any solid material depends on the presence of flaws. Since the number and severity of flaws likely varies between specimens, strength measurements for vertebrate tendons are also expected to be variable (Wainwright et al., 1982). Elliot (1965) reported tendon strengths ranging from 20 to 140 MPa. More recently, Bennett et al. (1986) measured the ultimate strengths of various mammalian digital and tail tendons using cryo-grips. Mean values ranged from 90 to 107 MPa, with a global mean across all species of about 100 MPa.

The high tensile stiffness and strength of tendon is attributed to its relatively high collagen content (70 to 80% dry weight; Elliot, 1965), and to its hierarchical organization into linear bundles. The majority of collagen fibres lie parallel to the long axis of the tendon, and the tropocollagen molecules in the heavily cross-linked regions of the fibres are crystallized, which together enhances the tensile properties of tendons. The multi-layered

fibre-bundle organization of tendon allows for the maintenance of high tensile strength, with considerable flexibility in bending, in the same way that wire rope maintains high tensile strength and flexibility as compared to an equal cross-section of solid steel, e.g., Alexander (1988a); Alexander (1988b) and Wainwright et al. (1982). Finally, the helical interweaving of the units varies among the structural levels, e.g., tropocollagen has a left-hand helix, while microfibrils have a right-hand helix, to keep the material from unwinding when loaded.

The significance of the observed tensile properties can be appreciated by considering tendon function. Tendon must be sufficiently stiff and strong to transmit muscle force to bone without being substantially deformed in the process. Ker et al. (1988) studied the relative size of muscle and tendon dimensions. They argued that thin tendons require long-fibred muscles, which allow for great changes in length, to compensate for tendon deformation during muscle contraction. In contrast, thick tendons deform less than thin tendons, and may not need extra-long fibres in the corresponding muscle. Ker et al. (1988) calculated an optimal ratio for the cross-sectional area of muscles and their associated tendons, based upon the isometric properties of mammalian striated muscle, and minimizing muscle-tendon mass. They found that in many mammalian species, including humans, the muscle tendon units approximated their calculated optimal ratio (Ker et al., 1988; Cutts et al., 1991). Minimizing body mass is an important aspect of the functional design of living systems.

If a tendon specimen is cyclically stretched and allowed to recoil within the range of reversible strain, the resulting load-deformation measurements form a loop (Figure 2.6.10). This result means that a proportion of the energy expended during tensile deformation of the tendon is not recovered when the deforming force is removed. The lost energy, or hysteresis, is quantified by considering the area enclosed within the loop. It is usually expressed as a percentage of the deformation energy (the area below the elongation curve). The reciprocal quantity, the resilience, is often used to describe the fraction of energy returned following tendon recoil.

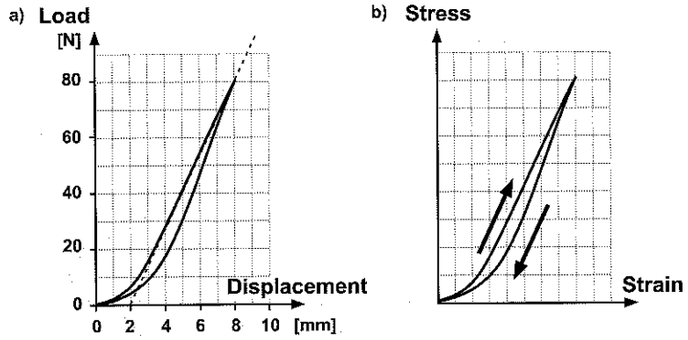

Figure 2.6.10 **(a) Load-displacement curve for a wallaby tail tendon. The dashed line represents the tangent modulus. (b) Typical stress-strain curve for tendon showing loading, unloading, and hysteresis loop (see text for further explanation) (from Bennett et al., 1986, with permission).**

Besides being relatively stiff and strong in tension, tendon is highly resilient. Ker (1981) reported that the hysteresis area of sheep plantaris tendon was about 6% of the area

under the loading curve, and that this value was effectively independent of frequency in the range of 0.2 to 11 Hz. Bennett et al. (1986) showed that mean values of hysteresis of several vertebrate tendons ranged from 6 to 11%, and were virtually independent of the frequency of loading. More recently, Wang et al. (1995) demonstrated that hysteresis is virtually unchanged up to test frequencies of 70 Hz. Thus, about 89 to 94% of the energy associated with longitudinal deformation or stretch of a tendon is recovered when the load on the tendon is removed. For a biological material, tendon shows marked elastic behaviour, at least within the likely range of physiologically relevant frequencies of deformation.

Depending on the function of its associated muscle, a tendon may be subjected to prolonged static loads, such as those imposed by postural muscles or prolonged repetitive or cyclic loads, such as those measured during locomotion. A material that fails under prolonged constant stress is said to suffer from creep failure (or rupture). Fatigue failure (or rupture) is the term used to describe the failure of a material subjected to prolonged cyclic loading.

Wang and Ker (1995) investigated the creep properties of wallaby tail tendon by subjecting uniform sections of tendons to static stresses ranging from 10 to 80 MPa. The specimens were immersed in saline-saturated liquid paraffin to prevent dehydration during the prolonged experiments. They found that the tendons suffered from creep rupture at tensile stresses that were much lower than those that caused failure during a single dynamic pull (Figure 2.6.11). Between 20 and 80 MPa, the time to creep rupture, or *creep lifetime*, decreased exponentially with increasing stress. Tendon specimens subjected to 10 MPa, however, showed no signs of creep damage even after 15 days, at which time the experiments were abandoned. Based upon estimates of the physiological cross-sectional area of wallaby tail musculature and estimates of maximum skeletal muscle stresses, Wang and Ker (1995) concluded that the tail tendons would be subjected to tensile stresses of about 14 MPa, and that it was unlikely that tail tendons would suffer from creep damage in the living animal.

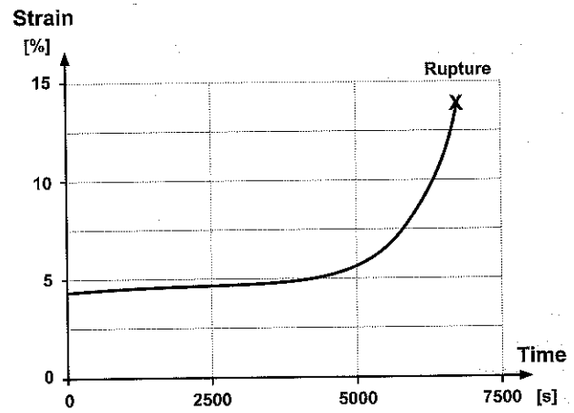

Figure 2.6.11 **Creep test. A load ramp was applied for the first 2 seconds. Thereafter, the stress was kept constant at 30 MPa until rupture. Wallaby tail tendon at 37°C. Specimen length was 150 mm (from Wang & Ker, 1995, with permission).**

In a companion study, Wang et al. (1995) subjected wallaby tail tendons to cyclic loading protocols to examine the potential for fatigue failure in these tendons. They found that the tail tendons suffered from fatigue rupture at stress levels that were much lower than those resulting in tendon rupture during a single dynamic pull. Additionally, dynamically-determined stiffness decreased gradually through each cycle of loading. They estimated that wallaby tail tendons would be subjected to about 14 MPa at a rate of about 3 Hz during moderately fast hopping (as the tail swings up and down in each stride), and calculated that the fatigue lifetime of the tail tendons would be about 56 hours. From these experiments, it seemed unlikely that tail tendons would fail due to fatigue damage. However, when Wang et al. (1995) tried to estimate the fatigue lifetime of the human Achilles tendon using their model and assumptions about typical stride frequencies and peak tensile stresses (about 1.4 Hz, as shown in Cavanagh & Kram, 1990), and 50 MPa (as shown in Ker et al., 1987), they concluded that fatigue failure should result after about one hour of continuous running. Clearly, Achilles tendons survive running times longer than one hour. Wang et al. (1995) suggested that despite the fact that mammalian tendons were virtually indistinguishable in terms of mechanical properties such as Young's modulus and resilience, highly stressed tendons, such as the Achilles tendon, may be more resistant to fatigue failure than tail tendons.

Because tendons are highly resilient structures, they are capable of storing and releasing significant amounts of elastic strain energy. This property of tendon is thought to be of considerable importance for the evolution of locomotor systems, particularly in high speed vertebrate locomotion such as that employed by ungulate mammals, i.e., those that walk on their toes, e.g., horses, deer, and camels. The proximal limb muscles of these animals are conspicuous for their large, multipennate, short-fibred structure, with long, cord-like tendons extending distally to the toes. When activated, these muscles are capable of generating large forces. However, because of their relatively short muscle fibre lengths, the active range of length changes in these locomotor muscles is limited. Therefore, part of the length changes in these muscle-tendon units is likely to occur within the tendons.

Alexander (1988a; 1988b) suggested that these types of locomotor muscles generate force to keep their corresponding tendons taut. Upon impact with the ground, these tendons are stretched and the energy associated with decelerating the mass of the animal during impact is stored as elastic strain energy in the tendons. During the propulsive phase of the stance phase, the tendons recoil, thereby, releasing part of the stored elastic strain energy. Alexander (1988b) proposed that the cyclic storage and release of elastic strain energy in tendon may be a mechanism for reducing the total amount of metabolic energy expended during locomotion. For this mechanism to work, metabolic energy is required to activate, and develop, tension in the proximal limb muscles. Short muscle fibres can exert as much force as an equal number of long muscle fibres. However, a muscle composed of short fibres is less massive, and, therefore, less costly to maintain and transport. Perhaps such a muscle is also less costly to activate. Alexander (1988b) hypothesized that high speed running in these animals has become more economical by virtue of having evolved muscles with short fibres and long tendons.

A more specific example that illustrates how the concept of elastic energy storage may be a mechanism for increasing the efficiency of high speed terrestrial locomotion is bipedal hopping of the kangaroos and their relatives (Macropodidae). Dawson and Taylor (1973) measured the oxygen consumption of kangaroos hopping on a treadmill. They showed that beyond a critical hopping speed, oxygen consumption leveled off, and in fact decreased slightly with increasing speed. Alexander and Vernon (1975) performed an analysis of the

mechanics of hopping with a wallaby (Macropus rufogriseus), a small species of kangaroo, by taking cinefilm recordings of animals hopping across a force platform. They found that most of the energetic demand of hopping at high speeds was associated with the gravitational potential energy (of the centre of mass of the whole body) and the horizontal component of the external kinetic energy (of the centre of mass of the whole body). Each of these forms of mechanical energy decreased with each impact (braking) and increased with each subsequent take off (propulsive). Alexander and Vernon (1975) also found that the lengthening phase of the ankle extensors (gastrocnemius and plantaris) coincided with the impact phase, and the shortening phase coincided with the take off phase. By assuming that most of the changes in length of the ankle extensor muscle-tendon units occurred within the tendon, rather than the muscle, Alexander and Vernon (1975) suggested that elastic strain energy storage during impact, followed by the energy release from these tendons during take off, may help to save metabolic energy. Further, they suggested that Dawson and Taylor's discovery could be explained by the increased role of storage of elastic strain energy at higher speeds of locomotion.

The role of tendon elasticity in human locomotion seems less certain than that in animal locomotion. Cavagna et al. (1964) estimated the mechanical efficiency of running humans. They found that the efficiency of running was greater than that of contracting an isolated muscle in the absence of any prestretch. They argued that during impact and take off, muscle-tendon complexes were stretched and relaxed, thus storing and releasing elastic strain energy. However, they were unable to differentiate between the potential for muscle strain energy and tendon strain energy. Van Ingen Schenau (1984) calculated the potential for elastic strain energy storage during running in humans. His calculations were based, in part, on the tensile properties of tendons and measurements of the ground reaction forces during running. Van Ingen Schenau (1984) argued that, compared to the total energy required to run, the amount of energy that could be saved by means of tendon elastic energy storage was insignificant.

Voigt et al. (1995) considered stationary bipedal hopping in an attempt to estimate the potential role of tendon elastic energy storage in the efficiency of human locomotion. Oxygen consumption was measured during three different speeds of hopping. High speed film and force plate analyses were used to calculate net joint moments, and standardized anatomical data were employed to estimate the instantaneous muscle-tendon unit forces for the knee and ankle extensors. Corresponding tendon stresses and strain energies were calculated using a standardized tendon stress-strain function and morphological data. Absolute work rates of the knee and ankle extensors were compared to the absolute work rate associated with the whole body during the hopping movements. Voigt et al. (1995) calculated that the quadriceps femoris and triceps surae tendons performed 52 to 60% of the total absolute work associated with stationary bipedal hopping, and that these tendons made greater contributions to hopping efficiency at hopping speeds that exceeded those individually preferred by each participant. It must be emphasized that the 52 to 60% of total work performed by the tendons found by Voigt et al. (1995) is absolute work. In reality, of course, the negative work required to stretch a tendon always exceeds the positive work the tendon can return. Therefore, the total work performed by a tendon during a loading-unloading cycle is always negative. Thus, while the role of tendon elasticity appears well-established for at least some vertebrate species, the debate continues as to the relevance of this mechanism during human locomotion.

The question may arise as to which scenario is metabolically more efficient: a tendon that is stretched (while the muscle fibres remain at constant length) or muscle fibres that stretch (while the tendon remains at constant length). An isometrically contracting muscle fibre (no change in fibre length) consumes more metabolic energy than an eccentrically contracting muscle fibre (actively lengthening fibre), for the same output of force. However, an isometrically contracting muscle fibre consumes less metabolic energy than a concentrically contracting fibre (actively shortening fibre), for the same output of force. A systematic investigation of the relative merits of the two extremes of very compliant muscle and very stiff tendon, and very stiff muscle and very compliant tendon, and the intermediate combinations, therein, has yet to be conducted. Until such time, the role of elastic energy storage in the enhancement of locomotor efficiency remains an intriguing question.

2.6.3 PHYSIOLOGICAL PROPERTIES AND ADAPTIVE FUNCTION

The glistening, white appearance of tendon gives the impression that it is an avascular (without blood vessels) structure. Certainly, relative to intensely metabolic tissues, such as muscle and skin, tendon vascularity is minimal. However, despite its macroscopic appearance, tendon is a metabolically active structure.

Although the blood supply to tendon is variable in volume and organization, in general, tendon vascularity, like tendon morphology, involves three regions: tendon, myotendinous junction, and osteotendinous junction. If present, vessels that perfuse the tendon originate from the paratenon or synovial fluid. Small blood vessels in the paratenon run transversely toward the tendon, and branch several times before running parallel to the long axis of the tendon. Vessels enter the tendon along the endotenon. Capillaries loop from the arterioles to the venules, but do not penetrate the collagen bundles. At the myotendinous junction, vessels surrounding the muscle fibres continue around the junction into the endotenon. The vessels do not cross the actual junction. Similarly, the blood vessels do not cross the osteotendinous junction, but are seen coursing around it, continuous between the periosteum and the endotenon (O'Brien, 1992).

While the major role of the blood supply is to perfuse the tendon fibroblasts with nutrients, the cells may also obtain nourishment by diffusion directly from the synovial fluid (Lundborg & Rank, 1978; Lundborg et al., 1980; Manske & Lesker, 1982). Synovial diffusion appears to be particularly important in areas of the tendon that are enclosed within synovial sheaths. The effectiveness of nutrient uptake by diffusion was compared to that by perfusion in flexor tendon cells of chickens (Manske et al., 1978) and primates (Manske & Lesker, 1982). Tritiated proline, the traceable radio-isotope of proline (an amino acid necessary for the synthesis of collagen), was taken up by the cells more completely and quickly via diffusion than via perfusion, indicating that diffusion was an effective mechanism for the supply of nutrients to tendon cells.

Tendon cells (tenocytes are the inactive form, and fibroblasts are the active form) are responsible for maintaining the metabolic balance of tendon. Tendon cell populations differ, depending upon location. For example, fibroblasts isolated from the surface of tendon, and subsequently cultured, adhered less well to the culture substrate than fibroblasts isolated from the tendon interior. Additionally, surface fibroblasts synthesized less glycosaminoglycans (ground substance molecules), and a limited amount (10%) of a mixture of collagen. The interior fibroblasts, in contrast, synthesized great amounts of glycosaminoglycans

(30%) and type I collagen (the main tendon-fibre collagen) (Reiderer-Henderson et al., 1983).

The biosynthesis of collagen is, arguably, the primary role of the tendon cells. In normal, healthy tendon, the rate of metabolism of collagen is slow. The fibroblasts produce the ground substance, into which they synthesize and deposit the tropocollagen molecules. At this early stage, there are no cross-links between the tropocollagen molecules. Tropocollagen cross-linking takes place around 4 to 16 days following the initial deposition of the molecules. During the next 12 weeks or so, the collagenous tissue becomes organized. Collagen fibres are formed, at first assuming a random orientation. Gradually, the randomly-oriented fibres come to lie parallel to the applied tensile loads (O'Brien, 1992). This reorientation enhances further cross-linking between the collagen fibres thus increasing the tensile stiffness and strength of the newly formed tissue.

The ground substance is not simply a *filler*, but has many important functions within the tendon. It is composed primarily of water, proteoglycan and glycoprotein macromolecules, and inorganic salts. A proteoglycan is made up of a protein core, with many large glycosaminoglycan (amino-sugar) side-chains. The long sidechains of these molecules can interdigitate with one another and form a web-like network. Glycoproteins are also protein-carbohydrate macromolecules, but with a predominant protein portion to which many small sugar molecules are attached. The sugar groups allow the macromolecules to bind large amounts of water by hydrogen-bonding. The combined macromolecular potential of binding large numbers of water molecules and forming extensive networks is responsible for the hydrated, gel-like consistency of the ground substance.

The ground substance provides the necessary structural support for the collagen fibres, and also serves as a lubricating medium, enabling fibres to slide with respect to one another during tendon movement. Additionally, it is thought that the substantial water content of the ground substance allows for considerable dissipation of energy in the form of heat during tendon function. This would seem to be particularly important in a tissue with relatively low vascularity, and, therefore, relatively low capacity for heat exchange by blood perfusion. Finally, the ground substance functions as a medium for the diffusion of nutrients and gases, particularly for cells located well away from blood vessels or synovial fluid (O'Brien, 1992).

Some of the ground substance macromolecules have been implicated in more specific roles. For example, fibronectin, a large glycoprotein, plays an important role in cell-cell adhesion, fibroblast to collagen attachment, and cell migration. It may also play an indirect role in the control of ground substance production (Viidik, 1990). The proteoglycans, e.g., decorin and biglycan, seem to be associated with the regulation of fibril formation, as the concentration of these proteoglycan molecules appears to be inversely proportional to the ultimate size of the tropocollagen (O'Brien, 1992).

Tendons are capable of detecting and responding to mechanical and biochemical changes within their physiological environment. If the rates at which these changes occur are not too great, and the absolute changes are not too extreme, then the tendon can adapt to the new conditions. However, if the mechanical or biochemical changes are rapid, severe, or prolonged in nature, the tendon may not be capable of repair. A considerable number of studies have been aimed at trying to determine the mechanical and biochemical conditions associated with successful tendon remodelling (or adaptive repair) and tendon injury.

Flint (1982) found that if the Achilles tendon of a rabbit was completely severed, the glycosaminoglycan content, the fibroblast number, and the number of small collagen fibres,

increased. The area of the tendon that was closest to the muscle belly showed the greatest changes, suggesting that tendon adaptation may be region-specific. If the severed tendon was sutured so that some tensile load could be transmitted, only minimal changes in glycosaminoglycan content and fibroblast and collagen fibre number, were observed. Thus, the removal of tension appeared to trigger tendon changes that were associated with collagen synthesis. In a study by Klein et al. (1977), the tensile forces normally associated with active muscle contraction were totally removed in the ankle extensor muscles of the rat by denervation (the surgical elimination of neural stimulation to the muscle). They observed dramatic increases in collagen turnover in the rat Achilles tendon, but did not observe changes in the relative amount of the various tendon components. It appeared that the tensile loads generated by the muscle had an important influence on collagen turnover.

Another way to change the mechanical environment of tendon is to increase the applied tensile load. Results from such studies are often difficult to compare because of the variable exercise regimes that were used to increase tendon load. For example, long-term running has been reported to increase the cross-sectional area and collagen content of swine extensor tendons. Similar changes were not observed in the flexor tendons of exercised animals (Woo et al., 1980; Woo et al., 1981). The differences in response of the extensor and flexor tendons to exercise were associated with different biochemical constituents and collagen concentrations, and different loading of flexor and extensor tendons during locomotion. Kiiskinen (1977) found that treadmill running appeared to cause an increase in the dry weight of the Achilles tendon in young mice. In senescent mice, however, treadmill running or voluntary exercise appeared to slow the age-related loss of glycosaminoglycans (Viidik, 1979; Vailas et al., 1985). In growing chicks, Curwin et al. (1988) observed that strenuous exercise slowed the maturation of collagen by increasing the turnover of ground substance and collagen. These results suggest that the response of a tendon to mechanical overload is tendon- and age-specific. Growth-related stimuli may conflict with exercise-related stimuli when growing animals are exercised. Furthermore, the stimuli responsible for tendon adaptation may change during maturation.

Over most of its length, tendon is loaded in tension. However, there are normal situations in which a tendon may be subjected to compressive loads. This occurs, for example, when a tendon passes around a bony prominence or turns through a digital sheath. Within this area, a specialized fibrocartilage *button* develops. The fibrocartilage button is like fibrocartilage that develops pathologically when a tissue that usually withstands tensile loads is experimentally subjected to compressive loads (Scapinelli & Little, 1970). Merrilees and Flint (1980) examined the ultrastructure of a rabbit flexor tendon. The rabbit flexor tendon is oriented such that tensile loads are sustained by the tissue along its superficial surface, while compressive loads are sustained by the tissue along its deep surface. The collagen in the tensile surface was oriented longitudinally, with typically elongated fibroblasts distributed among the collagen fibres. In contrast, in the deep zone of the tendon that was subjected to compressive loads, the collagen assumed a basket-weave orientation, and the associated cells resembled cartilage rather than tendon cells. The authors concluded that the observed differences in the morphology of the tendon between deep and superficial zones were caused by adaptive responses to the compressive and tensile loads.

Gillard et al. (1979) used the same rabbit tendon model as Merrilees and Flint (1980), however, they altered the loading pattern of the tendon by surgically relocating it, thereby, eliminating the compressive component of the load. Glycosaminoglycan content of the normally compressed region decreased by 60% within eight days of the removal of the compressive component. When the tendon was again subjected to the normal compressive component, the glycosaminoglycan content returned towards its previous level, albeit much more slowly than the rate at which the reduction occurred. These results support the notion that tendon is sensitive to the local loading environment, and that it is capable of responding to those changes in load by initiating changes in biochemical makeup and collagen orientation. In effect, tendon tissue becomes more cartilaginous in areas where it is subjected to compressive loads.

Tendon is capable of considerable self-healing, depending upon the type of injury. The most common tendon injuries are lacerations, ruptures, and tendinitis. The basic process of tendon healing may be considered to occur in three phases: inflammation with cellular infiltration, proliferation of new ground substance and collagen, and remodelling of the newly formed tissue. Lacerations and ruptures are considered to be acute traumatic injuries. Maintaining the blood supply to the healing tendon is critical to prevent necrosis of the collagen. However, maintaining blood supply may become problematic in areas of the tendon where vascularity is compromised because of friction, compression or torsion, e.g., in the Achilles tendon and the supraspinatus tendon. Another aspect of tendon healing that appears to affect the long-term result, particularly with injuries to the tendons in the hands, is the tendency for adhesions to form between the repair site and the tendon sheath. These adhesions may prevent the tendon from gliding easily within the sheath during joint motion. It has been suggested that maintaining contact between ruptured tendon ends (by prompt suturing), the early application of protected passive motion of the affected joint and hence, the injured tendon, and preventing adhesion formation between the injured tendon and its protective sheath, are the factors, which when combined, provide the best results for healing of tendon laceration and rupture (Gelberman et al., 1988).

Tendinitis (tendon inflammation), a common tendon injury most notably associated with pain, is often described as an overuse syndrome. Treatment protocols consist of pain management with the use of analgesics and anti-inflammatory agents to decrease the inflammation around the tendon. Physical agents, such as ice or ultrasound treatments, seem to be beneficial in the early stages of inflammation. It is suspected that the continuous cyclic loading of tendons causes microdamage, i.e., mechanical damage of the collagen fibres at the microscopic level. If the time frame between successive bouts of repetitive activity is sufficiently long, then the normal healing response can proceed and the fibroblasts can repair the microdamage. If the time frame is insufficient, the normal healing response will be initiated, but will not proceed beyond the inflammatory stage (Curwin & Stanish, 1984). While it is desirable to curtail activity that causes inflammation, it may be difficult to do so, particularly if the painful symptoms are work-related.

In an overload model of the rat plantaris tendon, Zamora and Marini (1988) found that there was a notable transformation of quiescent fibrocytes into active fibroblasts, without the presence of inflammatory cells. Collagen bundles in the tendon were disrupted, and empty longitudinal spaces were observed. Prompted by the observed ultrastructural changes, the authors suggested that the process of tendon remodelling may involve an initial transient period of mechanical weakness, and that the tendon breaks down structurally before remodelling. Unfortunately, the magnitudes of the overload, and the mechanisms by which the overloads contributed to the observed tendon changes, remain unknown (Archambault et al., 1995).

There seems to be a fine line between changes in the mechanical environment of a tendon (for example, magnitudes of the applied tensile loads and their respective time-

histories) that initiate the normal healing response and result in successful completion of an adaptive and remodelling process, and changes in the mechanical environment of a tendon that initiate the normal healing response, but instead terminate in chronic tendon inflammation. Backman et al. (1990) presented the first potentially quantifiable experimental model of overuse tendon injury. The goal of their experiment was to standardize the conditions relating to the development of chronic Achilles paratenonitis (paratenon inflammation) with tendinosis (degeneration of the tendon). Anaesthetized rabbits were exercised using a kicking machine for two hours per day, three days per week, for five to six weeks. Four weeks into the exercise protocol, the rabbits had noticeable nodules and thickening about 0.5 to 1.0 cm above the calcaneus. At the end of the exercise program, the paratenon of the exercised legs was visibly thickened and there was an increase in the number of blood vessels, edema, and infiltration of inflammatory cells. Most of the degenerative changes were seen centrally in the tendons (Figure 2.6.12).

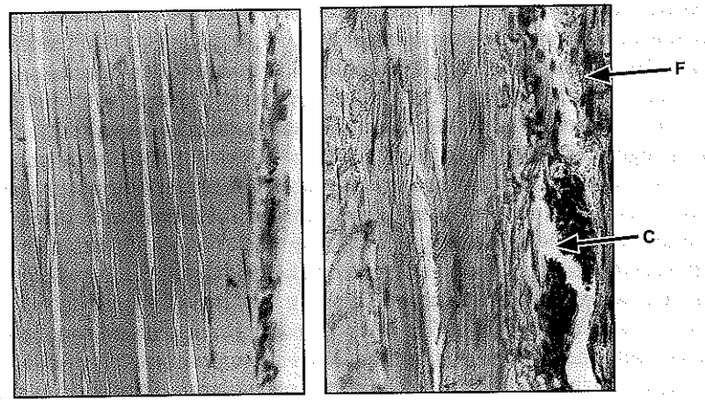

Figure 2.6.12 **Left: normal tendon and paratenon in control leg. Right: micrograph of exercised leg demonstrating fibrillation in tendon, dilated capillary (C), and increased number of fibroblasts (F) (from Backman et al., 1990, with permission).**

Archambault et al. (1997) developed a model for tendon overuse injury that built on the original model of Backman et al. (1990). Rabbits were exercised in kicking machines, and the tensile loads applied to Achilles tendons were recorded continuously (Figure 2.6.13). This model offers the possibility to correlate changes in the applied mechanical environment of the tendon with changes in the observed biochemical and physiological state of the tendon.

In the future, it may be possible to isolate the mechanical or temporal threshold, or both, of the tendon healing response, in which load-time histories below a threshold result in remodelling, and load-time histories above a threshold result in chronic inflammation.

2.6.4 TENDON-MUSCLE-APONEUROSIS INTERACTIONS

In section 2.6.2, we suggested that tendons play potentially important roles in modulating the length changes in fibres and fascicles, and in the storage and release of

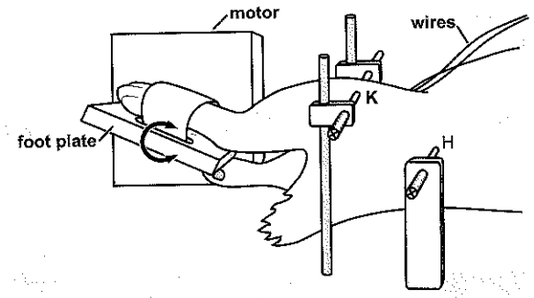

Figure 2.6.13 **Kicking machine (from Archambault et al., 1997, with permission).**

mechanical energy in cyclic movements. However, the examples only provided indirect evidence of the energy savings associated with the storage and release of energy, and did not directly tackle questions of how fibre length changes relate to the corresponding changes of the muscle tendon complex. Furthermore, the role of the aponeurosis as a potential site for energy storage was not considered.

When approaching the problem of energy savings through elastic elements in muscle, an important question that needs to be resolved is: are tendons and aponeuroses arranged in series, in parallel, or somewhere in between these two idealized states relative to the contractile muscle fibres? An argument frequently encountered in the biomechanics literature runs as follows: since the tendon and aponeurosis are structurally in series, they are also mechanically in series, and therefore sustain the same force, or at least, the forces they sustain are constantly in the same proportion. This reasoning has been used to measure the forces of a muscle at the distal end of the tendon, while recording elongations at some part of the aponeurosis, and then assuming that the two are related by a constitutive equation governing the (nearly) elastic behaviour of the aponeurosis, e.g., Magnusson et al. (2001) and Muramatsu et al. (2001). A good example of such reasoning, albeit made in a tacit fashion, has been put forward by Roberts et al. (1997). Similarly, van Ingen Schenau et al. (1997)) defined that the series elasticity of muscles is obtained simply by subtracting fibre length from the entire muscle tendon unit length, thereby explicitly including the tendon and aponeurosis as part of the series elasticity. Although there is little doubt that the tendon is arranged mechanically in series with the rest of the muscle, its arrangement relative to the aponeurosis is less obvious and cannot be easily discerned by casual analysis.

A frequently adopted model of series elasticity is shown in Figure 2.6.14, which represents a uni-pennate muscle with its associated contractile elements, tendon, and aponeuroses. Here, series elasticity (se) is depicted to reside in the fibres (f), the aponeuroses (a), and tendon (t). Although, there is little doubt that both tendon and aponeuroses might affect length changes of the fibres, for questions related to energy storage and release, as well as efficiency, the role of the aponeurosis in terms of force transmission needs clarification.

There are observations indicating that aponeuroses are not mechanically arranged in series with the muscle contractile elements or the tendon, or both. For example, Zuurbier et al. (1994) found that aponeurosis segment lengths decreased when a muscle was activated (and force increased), while Lieber et al. (2000) found that aponeurosis length depended on the

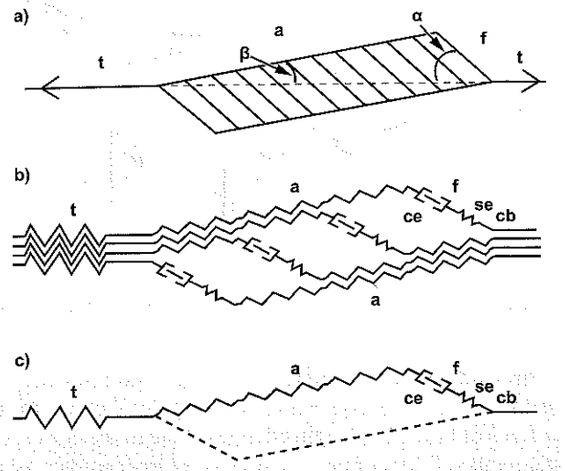

Figure 2.6.14 **Schematic illustration of a uni-pennate muscle with fibres (f), tendons (t), and aponeuroses (a). The angle of pennation between the line of action of the muscle and fibres (α) and the angle between the aponeurosis and the line of action (ß) are also shown. (b) Schematic illustration of the perceived series elastic elements (zig-zag lines) in the fibres, tendon and aponeuroses. (c) The corresponding series elasticity associated with a single fibre including the aponeurosis and tendon (from Ettema and Huijing, 1990, with permission).**

state of activation. Specifically, for a given amount of force acting on the distal tendon of a muscle, aponeurosis length was smaller when force was produced actively by the muscle compared to when force was passively applied to the muscle.

To clarify the role of aponeuroses in force transmission from fibres to the tendon, and to determine if aponeuroses are arranged mechanically in series with the tendon or muscle fibres, or both, we isolated the cat medial gastrocnemius muscle (MG) at its distal end with a remnant piece of the calcaneus bone still attached to the tendon. Otherwise, the muscle was left in its in situ configuration, with blood and nerve supply intact. The distal end of the muscle was attached to a muscle puller for computer controlled length changes of MG and for force measurement. The muscle was activated through tibial nerve stimulation (Herzog & Leonard, 1997) and tendon, aponeuroses and fibre length were measured using sonomicrometry (1997), with a crystal arrangement as shown in Figure 2.6.15.

When pacing the muscle through various work loop conditions (stretch-shortening cycles at various frequencies and magnitudes), it could be observed that some aponeurosis segments shortened when muscle force increased, and elongated when force decreased (Figure 2.6.16a - dashed vertical lines). This result indicates that aponeurosis length changes were not directly related to muscle force, and that force transmission from the muscle fibres to the aponeurosis was much more complex than could be explained with an idealized in series arrangement of fibres with the aponeurosis. When plotting the corresponding muscle force as a function of the aponeurosis segment length, the resulting loop ran in the counter-clockwise direction (Figure 2.6.16b). If this result was interpreted (incorrectly) as

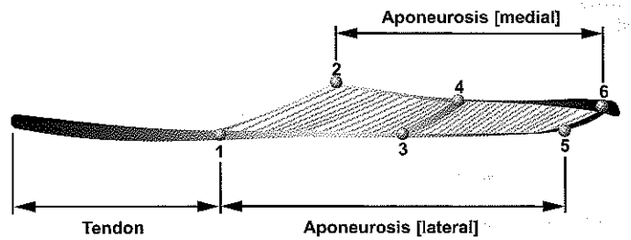

Figure 2.6.15 **Schematic illustration of the cat medial gastrocnemius muscle with the placement of six sonomicrometry crystals for measurement of fibre and aponeuroses segment lengths.**

a work loop of the aponeurosis, it would indicate that the aponeurosis produces net work during a full cycle, which is impossible for a (visco-) elastic tissue.

Roberts et al. (1997) studied the work contribution of the tendon and aponeuroses to the total work in the lateral gastrocnemius of running turkeys. They measured the total muscle length and fibre length and assumed implicitly that the difference between muscle and fibre length gave the length of an in series elastic element, as had been proposed by others (van Ingen Schenau et al., 1997). They found that the aponeurosis contributed as much as 60% of the total work in the shortening phase of the muscle, while the contractile contribution was about 40%. Their results cannot be properly evaluated, as data for full step cycles were not given. However, when applying identical methods to elucidate the role of the aponeurosis and tendon in the cat MG during free locomotion, we found that muscle force was primarily associated with the stance phase of gait, while the swing phase occurred essentially passively. However, muscle length changes during the stance phase of galloping were in the order of 10mm, while MG fibres remained at a nearly constant length (Figure 2.6.17a). If we now associate tendon/aponeurosis length changes with MG force by subtracting fibre lengths from muscle tendon unit length, as suggested by others (van Ingen Schenau et al., 1997; Roberts et al., 1997), while carefully accounting for any changes in the angle of pennation, the net mechanical work associated for a full step cycle (from zero force back to zero force) would be positive. In the example shown (Figure 2.6.17b), the net mechanical work associated for a full step cycle would account for more than 80% of the total work produced by MG, illustrating again that muscle force cannot be assumed to be transmitted along the MG aponeurosis in an in-series mechanical arrangement. This result was confirmed when the directly measured length of the distal segmet of the medial aponeurosis (crystals 2-4; Figure 2.6.15) was plotted as a function of the directly measured MG force. The resulting loops for all step cycles were counter-clockwise (Figure 2.6.18).

The conclusions drawn from these experiments are as simple as they are important. Aponeuroses of muscles must not be assumed to be arranged mechanically in series with either the muscle fibres or the tendon. Any such assumption needs careful justification in each case, and published literature on aponeuroses stiffness (or other mechanical properties) and the contributions of tendons/aponeuroses to the storage and release of elastic energy need careful evaluation, specifically if aponeurosis length changes (and, therefore, storage and release of energy in aponeuroses) are directly related to muscle forces.

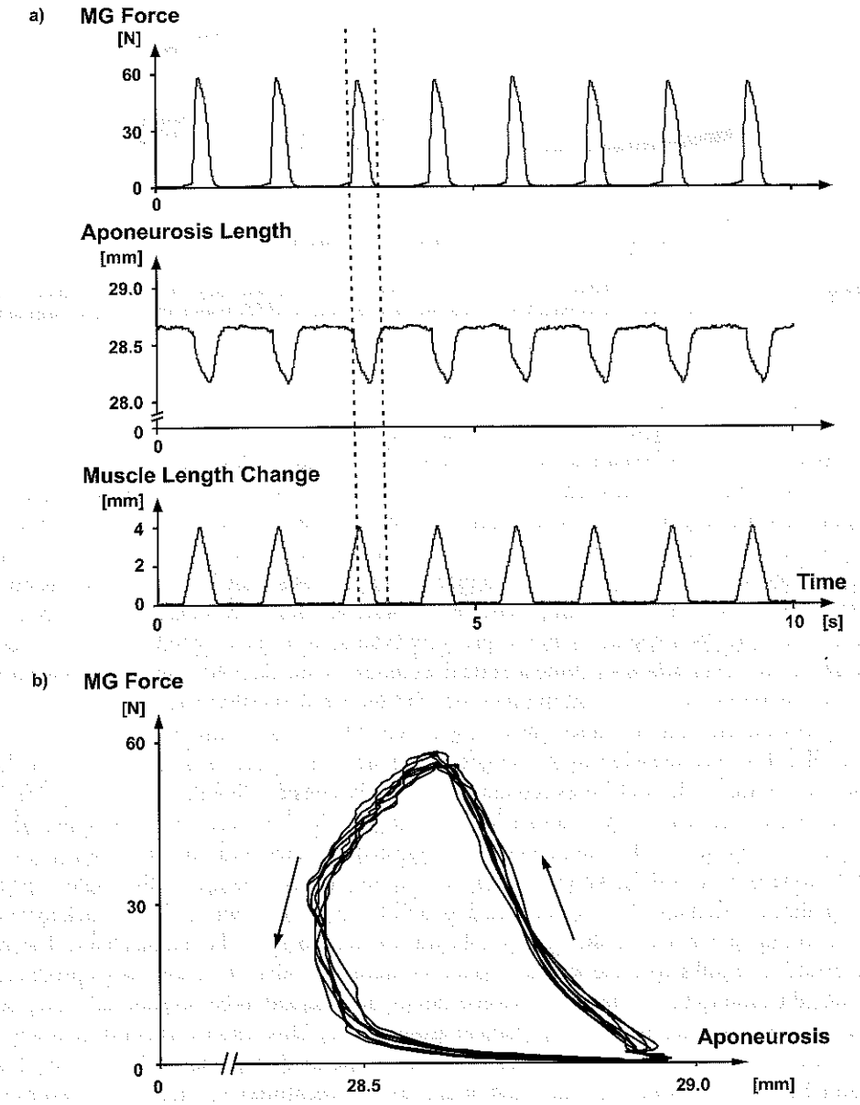

Figure 2.6.16 (a) Force-time, aponeurosis segment length-time, and muscle length change-time for work-loop experiments with cat medial gastrocnemius. Note that upon force production, the aponeurosis segment length decreases. (b) Medial gastrocnemius vs. aponeurosis segment length plots for the work loop experiments shown in (a). Note that the force-length plots run counter-clockwise, which would mean that the aponeurosis segment produces net mechanical work (which is impossible!), if it was assumed to be arranged mechanically in series with the tendon.

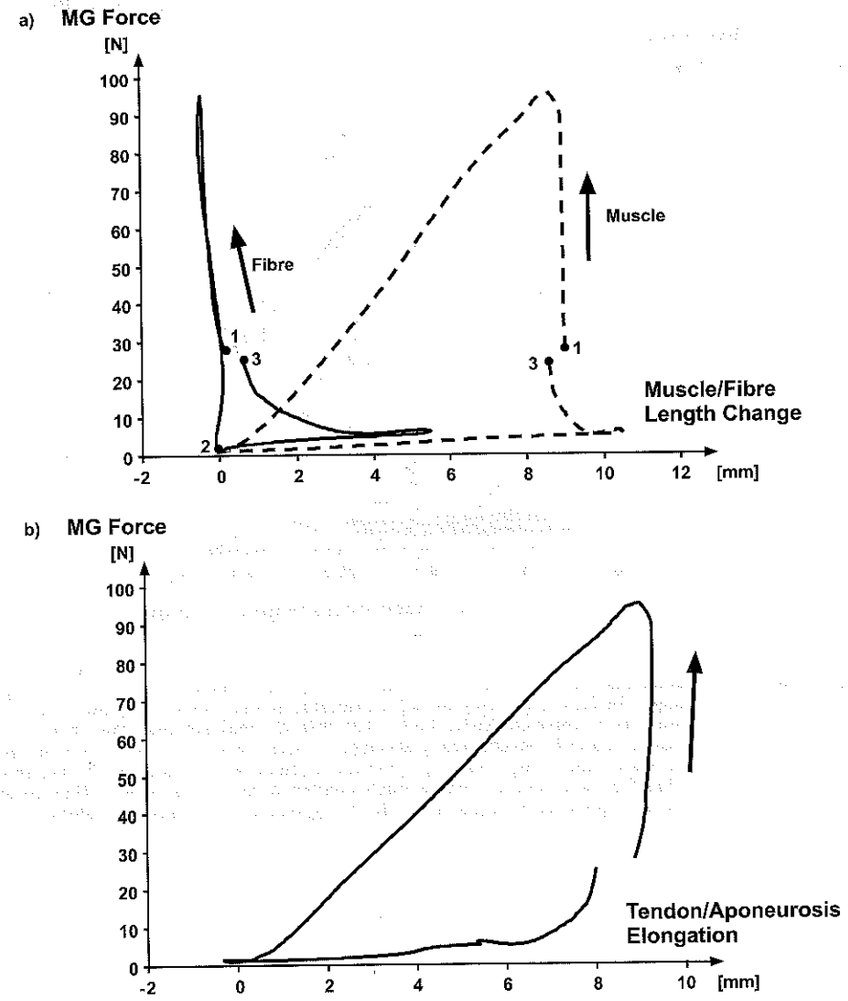

Figure 2.6.17 (a) Medial gastrocnemius force as a function of muscle (dashed line) and fibre (solid line) length change for a single step cycle of a cat galloping at 4 m/s on a 10° uphill slope. Note that during the stance phase of the step cycle (from label 1 to 2), the muscle shortens by almost 10mm, while fibre length remains virtually constant. (b) If we now plot MG force as a function of tendon/aponeurosis elongation in the way proposed by van Ingen Schenau et al. (1997) and Roberts et al. (1997), we obtain a work-loop that runs counter-clockwise. Again, we have to realize that the tendon (where MG force is measured) is not mechanically arranged in series with the aponeurosis, otherwise, we would (erroneously) associate a great amount of net mechanical work with the aponeurosis segment.

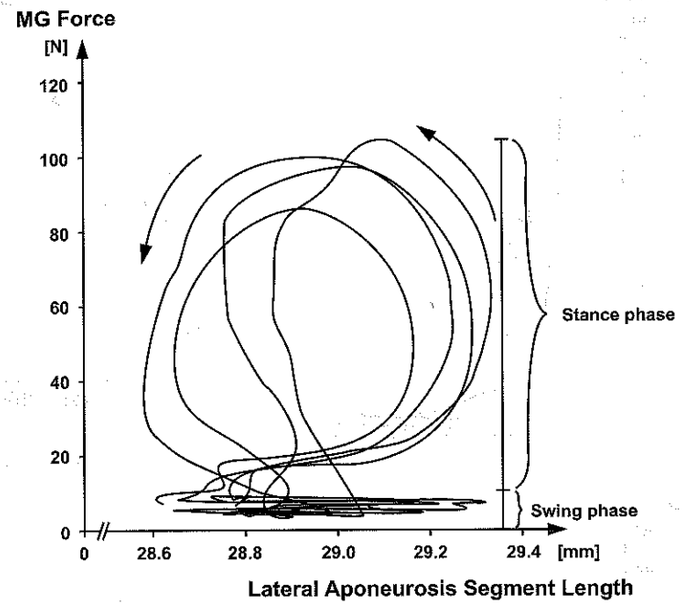

Figure 2.6.18 **Medial gastrocnemius force as a function of lateral aponeurosis segment length changes for four step cycles during cat running at 4 m/s on a 10° uphill slope. Note again, the counter-clockwise loops that directly indicate that the aponeurosis segment cannot be mechanically arranged in series with the tendon. Note further that during the swing phase aponeurosis segment length changes are like those during the stance phase, despite much smaller forces, demonstrating that muscle force and aponeurosis segment length are not related in an in series fashion.**

2.7 MUSCLE

HERZOG, W.

2.7.1 INTRODUCTION

Probably the most basic property of muscle is its ability to produce force. However, despite centuries of research on muscle and its contractile behaviour, some aspects of muscular force production have still not been resolved. For example, the precise mechanism of cross-bridge attachment and cross-bridge movement that are believed to cause relative movements of the myofilaments, and so produce force, are not clearly understood. Some scientists, e.g., Iwazumi (1978) and Pollack (1990), propose mechanisms of force production that do not agree with the most popular paradigm of muscular force production, the Cross-bridge theory (Huxley, 1957; Huxley & Simmons, 1971; Huxley, 1969; Rayment et al., 1993a). In this chapter, muscular force production and the mechanical properties of muscles are associated with the assumptions and predictions underlying the Cross-bridge theory. However, be aware, at all times, that not all of these assumptions and predictions have been tested and accepted unanimously in the scientific community.

Since this book is aimed at the student of biomechanics, muscles are viewed from a mechanical point of view. However, because of its contractile properties, muscle is less easily associated with strictly mechanical properties than are bones or ligaments, which have well-defined force-elongation or stress-strain relations. When dealing with the mechanics of muscle, muscle's physiological and biochemical properties must always be kept in mind.

Muscles exert force and produce movement and therefore may be considered the basic elements of movement mechanics in humans and animals. At the same time, force-time histories of muscles during movements are like small windows to the brain that may produce insight into the mechanisms of movement control. It is precisely the duality of mechanics and control function that splits biomechanists into two groups:

- Those who study the force output of muscles to determine the movement and loading effects on skeletal systems, in particular on joints, and
- Those who determine the force output of muscles for varying movement conditions to study the possible mechanisms that may be responsible for movement control.

This chapter focuses on muscle morphology and structure. In combination with the Cross-bridge theory, muscle morphology and structure determines, to a large extent, the mechanical properties of muscles.

2.7.2 MORPHOLOGY

Morphology is the science of structure and form without regarding function. This chapter demonstrates that muscle is a highly structured and organized material—every structure and each organization may be associated with specific functional properties of muscle.